JUNE 2016

M.Sc. in Civil Engineering

MOHAMMED AMER KAMIL

UNIVERSITY OF GAZİANTEP

GRADUATE SCHOOL OF

NATURAL & APPLIED SCIENCES

HIGH STRENGTH GLASS FIBER REINFORCED CONCRETE (GFRC) CORBELS

M.Sc. THESIS

IN

CIVIL ENGINEERING

BY
MOHAMMED AMER KAMIL
JUNE 2016

High Strength Glass Fiber Reinforced Concrete (GFRC) Corbels

University of Gaziantep

M.Sc. Thesis

in

Civil Engineering

Supervisor

Prof. Dr. Abdulkadir ÇEVİK

Co-Supervisor

Assist. Prof. Dr. Mehmet Eren GÜLŞAN

By

Mohammed Amer KAMIL

June 2016

REPUBLIC OF TURKEY
UNIVERSITY OF GAZİANTEP
GRADUATE SCHOOL OF NATURAL & APPLIED SCIENCES
CIVIL ENGINEERING DEPARTMENT

Name of the thesis: High Strength Glass Fiber Reinforced Concrete (GFRC) Corbels

Name of the student: Mohammed Amer KAMIL

Exam date: June 13, 2016

Approval of the Graduate School of Natural and Applied Sciences

Prof. Dr. Metin BEDİR

Director

I certify that this thesis satisfies all the requirements as a thesis for the degree of Master of Science

Prof. Dr. Abdulkadir ÇEVİK

Head of Department

This is to certify that we have read this thesis and that in our consensus/majority opinion it is fully adequate, in scope and quality, as a thesis for the degree of Master of Sceince.

Assist. Prof. Dr. Mehmet Eren GÜLŞAN

Co-Supervisor

Prof. Dr. Abdulkadir ÇEVİK

Supervisor

Examining Committee Members:	Signature
Prof. Dr. Abdulkadir ÇEVİK	.....
Asst. Prof. Dr. Nildem TAYŞİ	.....
Asst. Prof. Dr. Şafak Hengirmen TERCAN	.....

I declare that all information in this document has been obtained and presented in accordance with academic rules and ethical conduct. I also declare that, as required by these rules and conduct, I have fully cited and referenced all material and results that are not original to this work.

Mohammed Amer KAMIL

Signature

ABSTRACT

HIGH STRENGTH GLASS FIBER REINFORCED CONCRETE (GFRC) CORBELS

KAMIL, Mohammed Amer
M.Sc. in Civil Engineering
Supervisor: Prof. Dr. Abdulkadir ÇEVİK
Co-Supervisor: Assist. Prof. Dr. Mehmet Eren GÜLŞAN
June 2016
65 pages

The aim of the thesis is to investigate the effect of glass fiber on the mechanical behavior of reinforced concrete corbels. This study is the first experimental investigation that describes the behavior of high strength glass fiber reinforced concrete corbels. A total of 9 double sided corbels has been made of high strength concrete with a compressive strength of approximately 100 MPa. These specimens were loaded with vertical load until failure in which the shear span, and the fiber percentage were varied. All corbels have the same size and reinforced with the same main reinforcement. Test results show that the addition of glass fiber to the specimens enhanced the bearing capacity of corbels and improved the ductility remarkably. The cracking of glass fiber reinforced specimens were slower compared to the plain specimens, moreover, the fibrous corbels has much smaller crack width as compared to corbels without glass fiber this reduction leads to long service life which a desirable characteristic in corbels design. However, the mode of failure of corbels was sudden even after the addition of glass fiber. In addition, the results indicate a significant reduction in the strength of the specimens with and without glass fiber as the shear span increased.

Keywords: Glass Fiber Reinforced Concrete, Corbels, Load Bearing Capacity, Ductility, Failure Mode, High strength concrete corbels.

ÖZET

CAM LİF KATKILI YÜKSEK MUKAVEMETLİ BETONARME KISA KONSOLLAR

KAMIL, Mohammed Amer
Yüksek Lisans Tezi, İnşaat Mühendisliği
Tez Yöneticisi: Prof. Dr. Abdulkadir ÇEVİK
Yardımcı Tez Yöneticisi: Yrd. Doç. Dr. Mehmet Eren GÜLŞAN

Haziran 2016
65 Sayfa

Bu tezin amacı cam liflerin yüksek mukavemetli betonarme kısa konsolların mekanik davranışı üzerindeki etkisini araştırmaktır. Bu çalışma cam lif katkılı yüksek mukavemetli kısa konsolların davranışını araştıran ilk deneysel çalışmadır. Toplamda 9 adet basınç mukavemeti değeri yaklaşık 100 MPa olan çift kollu cam lif katkılı yüksek mukavemetli betonarme kısa konsol üretilmiştir. Bu kısa konsollar, net açıklık ve lif oranı değiştirilerek göçme oluşuncaya kadar dikey olarak yüklenmiştir. Bütün kısa konsollar aynı boyuttadır ve aynı donatı oranına sahiptir. Deney sonuçları, numunelere cam lif eklenmesinin yük taşıma kapasitelerini ve sünekliklerini önemli derecede geliştirdiğini göstermektedir. Çatlak oluşumu cam lif katkılı numunelerde düz betonarme olan numunelere göre daha yavaş oluşmaktadır. Ayrıca, cam lif katkılı kısa konsolların göçmeden sonraki çatlak genişliklerinin cam lif katkılı olmayan numunelere kıyasla daha küçük olduğu gözlemlenmiştir. Bu durum kısa konsol tasarımında istenen bir özellik olan uzun servis ömrünü sağlamaktadır. Ancak, cam lif katkılı olsa bile kısa konsolların göçmesi ani olmaktadır. Ayrıca deney sonuçları net açıklık artışının hem cam lif katkılı hem de cam lif katkısız numunelerde önemli bir yük taşıma kapasitesi kaybına neden olduğunu göstermiştir.

Anahtar Kelimeler: Cam Lif Katkılı Beton, Kısa Konsollar, Yük Taşıma Kapasitesi, Süneklik, Kırılma Modu, Yüksek Mukavemetli Kısa Konsollar

This thesis is dedicated to my parents.

ACKNOWLEDGEMENTS

First I offer my sincerest gratitude to my supervisor Prof. Dr. Abdulkadir ÇEVİK for all his help and guidance in every step of my research. His great personality and level of knowledge has been a constant source of inspiration for me. He consistently allowed this thesis to be my own work, but steered me in the right the direction whenever he thought I needed it.

I would also like to sincerely thank my co-supervisor Asst. Prof. Dr. Mehmet Eren Gülşan for his help and guidance without him this thesis would not have been completed.

I would also like to thank all people who helped me during my experimental works. I might not complete my experimental works without their devoted support.

Finally, I must express my very profound gratitude to my parents for providing me with unfailing support and continuous encouragement throughout my years of study and through the process of researching and writing this thesis.

TABLE OF CONTENTS

LIST OF FIGURES

Page

LIST OF TABLES

Page

LIST OF SYMBOLS

a	Shear span of corbels
A_n	extra main steel provided for horizontal loads.
A_s	Cross sectional area of main reinforcement
A_{vf}	area of reinforcement that crosses that assumed shear plane.
b	Width of corbel
d	Effective depth for corbels
h	Height of corbel
f_c	Cylindrical compressive strength of concrete
f_{cu}	Cubic compressive strength of concrete
f_{st}	Splitting tensile strength of concrete
f_t	Tensile strength
f_y	Yield strength of main reinforcement
n	Ratio of the elastic modules of steel and concrete
v_f %	Glass fiber percentage amount
V	Load carrying capacities of corbels
ρ	Reinforcement ratio
ϕ	Capacity Reduction Factor

θ The inclination of compression strut to tension tie.

μ the coefficient of friction

CHAPTER 1

INTRODUCTION

1.1 General

Corbels are structural elements normally used in reinforced concrete structures and particularly in precast reinforced concrete elements which their main function is to transfer the vertical and horizontal forces to the principal members.

Corbels transfer loads from primary beams and girders to columns. This means that corbels are subjected to high concentrated loads, and thus, can be classified as "disturbed regions". For many years engineers have been trying to find rational methods to analyze and design disturbed regions. Strut and tie models have been developed and refined over the years to become a very powerful tool in the design and analysis of corbels.

Therefore improving the design of corbels is a worthwhile goal towards achieving durable, serviceable, and safe precast concrete structures. Structural members, of precast pre-tensioned concrete structures, should be designed to support service loads without cracks or with minimal crack widths. In order to achieve this, the designer should consider improving the quality of concrete and performing a crack prevention design.

In these elements, the existence of high values of shear forces reduces their flexural capacity. Moreover, in the presence of cyclic actions or when high strength concrete is utilized, further penalization occurs in complete flexural capacity and ductility (Campione, 2005).

Corbels are characterized by a shear span-depth ratio (a/d) normally lower than unity and subjected to concentrated forces as in the support zones. For these reasons, they are host zones of static and geometric discontinuities and the hypothesis assumed for members in flexure that sections remain plane after deformation is not valid in this case.

High strength concrete has received wide recognition in recent years, due to major advantages of permitting a reduction in structural element; it provides higher stresses and increases the modulus of elasticity resulting in less deflection; it has a greater tensile strength which is beneficial in prestressed concrete construction, and its reduced tendency to creep results in a smaller long-term deflection and loss of prestress.

From 1980 onward, the application of high strength concrete has steadily increased to cover all aspects of structural construction such as high-rise buildings, bridges, columns, piles etc.

1.2 Glass Fiber Reinforced Concrete (GFRC)

Strengthening cement by adding fibers dates back to 1908 when cement entered the market. The composition of fiber and cement became a major constructional product because it overcame the main weakness of cement products brittleness. Reinforced concrete depends on upon the addition of continuous reinforcement such as steel rebar or welded wire fabric, to give it necessary tensile strength. However, obtains strength from dispersed tiny fibers, so that making thin board products, shingles, siding, pipe and a number of other products is possible (NEAL, 1978).

Scientists made an evaluation of a number of fibers, including carbon steel, stainless steel, carbon, various plastics, rock wool, and glass. The success of glass fiber as a reinforcement had made glass fiber mixed into cement and concrete look like a winner. Researchers struck out when they first tried this, however. Test samples were initially strong but the strength dropped off as the samples aged because the highly alkaline environment provided by cement attacked surfaces of the glass fibers.

In 1971, scientists at Pilkington and the Building Research Establishment, also in England, announced joint development of an alkali-resistant glass fiber. In the U.S., Owens-Corning had developed an alkali resistant fiber concurrently. The two firms subsequently worked out a technology exchange and both are doing continuing research on the fibers (NEAL, 1978).

The addition of glass fibers to the reinforced concrete has many advantages it helps to produce a thin, lightweight, yet strong structural member. High compressive and

flexural strengths, ability to reproduce fine surface details, low maintenance requirements, low coefficients of thermal expansion, high fire resistance, and environmentally friendly made GFRC the ideal choice for civil engineers. The strength of GFRC is determined by glass content, fiber size, fiber compaction, distribution, and orientation.

Figure 1.1 Short glass fibers

1.3 Research Significance

The main motivation of this study was to develop GFRC corbels for building construction with precast elements. Most of the precast structural elements consisted of corbels. However, the composition of GFRC matrix was varied. Fly ash and silica fume were added to the mixture to improve the strength and durability characteristics. Chopped glass fibers in addition to steel bars with a diameter of 8mm were selected for reinforcement.

Many studies have been carried out about corbels. However, these studies were focusing on the characteristics of the plain concrete or concrete reinforced with steel bars. Many researchers have expanded in the area of fiber reinforcement with steel fibers , though, little amount of studies focused on the applications of adding chopped glass fiber to corbels as a means to enhance the tensile strength and ductility of these structural members. Therefore, this research is important to expand the information about concrete corbels reinforced with glass fibers performance through experimental investigation and results analysis, In order to overcome the lack of information in this field, this study is required.

1.4 Research Objectives

In this research, experimental work has been carried out on plain and glass fiber reinforced concrete corbels. A wide range of physical models for analysis of corbels has been studied**.**

This thesis is devoted to study the mechanical properties of concrete corbels reinforced with glass fibers and the associated properties of GFRC. The main objectives are as follows:

- To study the ultimate strength and load-deformation characteristics of concrete corbels reinforced with glass fiber and steel reinforcement.
- To compare the crack control properties of glass fibers with concrete without glass fibers.
- To predicate the failure type of GFRC corbels.
- To conduct tests on full-scale corbels utilizing reinforcement bars and fibers.
- To assess the effects of shear span-depth ratio and of reinforcement content on the above characteristics.

1.5 Thesis Layout

The thesis was planned to provide additional knowledge on the structural behavior of corbels under vertical loading and with and without glass fiber reinforcement, by carrying out suitable series of tests.

In Chapter 2, the literature review for GFRC was presented. In addition to the previous studies made about fibrous reinforced concrete corbels and corbels design.

In chapter 3, Details of materials and their properties were presented, which were used in this experimental investigation. The mix proportions used and details of the experimental program are also given in the same chapter.

Chapter 4 gives the experimental results and shows the response of the tested corbels and discuss the cracking patterns and the effect of glass fiber addition to concrete corbels.

In Chapter 5, conclusions are presented with recommendations for further studies.

CHAPTER 2

LITERATURE REVIEW

2.1 Fiber Reinforced Concrete

Fiber Reinforced Concrete (FRC) is widely used due to the high corrosion resistance, high ductility, and sufficient durability. FRC is used in many structural fields especially in the military and marine fields, for instance, in fortified structures, blast resistant structures, offshore platforms, the exploitation of undersea oil engineering, etc. (Najim, 2002).

The addition of fiber to the concrete can improve the characteristics of the concrete such as the tensile, flexural, impact, fatigue and abrasion strength, deformation capability, toughness and load bearing capacity after cracking (Mohammadi et al., 2008).

There are several types of fiber can be used in cement and concrete composite, such as steel or carbon or glass fibers. Among all the used fibers currently, steel fiber has many advantages such as high elastic modulus and stiffness. Therefore, the addition of steel fiber significantly improves the compressive strength and toughness of concrete. However, the main disadvantage of steel fiber it can be rusts easily. Although, the addition of steel fiber to the concrete will increase the structure weight of the concrete and will cause a balling effect in mixing, and thus the workability will be lowered (Nanni, 1991).

Glass fibers are relatively inexpensive, lightweight and have high tensile strength. Studies have shown that the addition of glass fibers in concrete can control shrinkage cracking, improve the flexural and tensile strengths and also increase the post-peak ductility in compression (Tassew and Lubell, 2014). The main disadvantage of glass fiber has high sensitivity to alkaline conditions (Deák and Czigány, 2009).

2.2 Glass Fiber Reinforced Concrete

There are many researchers investigated the effect of adding glass fiber to the concrete mix. These researchers present previous experimental and theoretical studies. One of these studies was made by Shakor and Pimplikar (2011). In their study they aimed to indicate the differences in compressive strength and flexural strength by making tests using cubes with deferent sizes (150x150x150) mm and (100x100x100) mm, based on the test results, they noticed that when they used 1.5 % of glass fibers the average compressive strength of concrete is maximum. But with lower or higher percentage of glass, reduction in the strength was observed by 15% to 20%. They concluded that cohesiveness between the particles of concrete affected by increasing the weight of glass fiber, this can cause reduction in compressive strength, flexural and tensile strength. The test results showed there is compatibility between the glass fiber and concrete which helps to use it easily in our daily project especially for the facade of buildings, glass fiber that has good resistance to alkalinity that contains in cement (pH > 12.3) with high level. In their study, they stated that only 10 mm coarse aggregate should be used to solve the problem of reduced flexural strength. Lastly glass fiber can control shrinkage cracks easily; it shows this property particularly in cladding purpose or rendering. Because of most important thing in GFRC, it is water: cement ratio maximum 0.35, which helps to control the shrinkage and bonding each other by glass fiber.

The mechanical behavior of ultra-high strength reinforced concrete with glass fiber (UHS-GFRC) was studied by Roth et al. (2010). The study presents an understanding of the tensile failure characteristics and their relationship to flexural response.by making third-point bending experiments, direct tension experiments, and finite element analyses were used to study the material's responses under various loading conditions.

Flexural experiments showed that the thin UHS-GFRC panels' load-displacement response was essentially bilinear up to ultimate load with a mean initial elastic stiffness of 5.7 × 106 psi (39.3 GPa), or approximately twice that of typical concrete. The flexural experiments also indicated that the material's first crack strength, which coincided with the transition point in the load-displacement response, was approximately 1900 psi (13.1 MPa), or 8.8% of the unconfined compressive strength.

After the first crack transition from initial linear- elastic to deflection-hardening response occurred, the panel stiffness decreased by approximately 85% to a value of 0.8 × 106 psi (5.5 GPa), whereas an average overall increase in load capacity of approximately 33% prior to ultimate failure was observed. Displacement at ultimate failure was observed to be the property of greatest variability, with a range of 0.831 to 0.268 in. (21.1 to 6.8 mm). The expected cause of this large range of ultimate displacements was the stochastic distribution, orientation, and concentration of the glass fibers.

The primary concern for glass fiber reinforced cement composites (GFRC) is the durability of glass fibers in the alkaline environment of cement, Marikunte et al. (1997) presented experimental study on the hot-water durability of glass fiber reinforced cement composites. Glass fibers and pozzolanic materials such as silica fume and fly ash were used in the mix. Hot water durabilities of AR-glass fiber reinforced composites in blended cement matrix were compared for their flexural and tensile performance. Specimens after normal curing of 28 days were immersed in a hot water bath at 50°C for up to 84 days and then tested in flexure and tension. The results of the experimental study showed that the addition of glass fibers to the cement matrix significantly improves the flexural and tensile behavior of cement matrix. However, the performance of these composites with aging depends on the matrix mix ingredients. Synthetic pozzolan significantly improved both the flexural and the tensile behavior of aged GFRC composites.

Choi and Yuan (2005) studied the effect of adding glass fiber and polypropylene fiber on the splitting tensile strength and compressive strength of reinforced concrete. The fiber amounts were used 1.0% and 1.5% of the mixed concrete by volume. They made 18 cylinder specimens from each mix for compression and splitting tensile tests. The tests at 7, 28 and 90 days were made. Test results indicate that the addition of glass and polypropylene fibers to concrete increased the splitting tensile strength of concrete by approximately 20–50%, and the splitting tensile strength of GFRC and PFRC ranged from 9% to 13% of its compressive strength. Based on this investigation.

A similar trend was observed by Chandramouli et al. (2010). He investigated GFRC compressive, split tensile and flexural strength, Test specimens consisting of 150×150×150 mm cubes, 150×300 mm cylinders, and 100×100×500 mm beams were

cast. The compressive strength of GFRC was increased by 20 to 25 % and the increment percentage of flexural and split tensile strength of GFRC were 15 to 20%.

Kizilkanat et al. (2015) made comparative experimental investigation between basalt and glass fibers as fiber reinforcement in high strength concrete. In this study, it was reported that by adding glass fibers to the concrete mix the workability of concrete decreased. The results of the tests showed that the addition of fiber content greater than 0.25% resulted in slight increase in compressive strength. GFRC showed the highest compressive strength of 67.6 MPa at 0.75% inclusion. While BFRC showed the highest compressive strength of 66.6 MPa at 0.50% inclusion, whereas in comparison the compressive strength of plain concrete was 63.4 MPa. He observed there no increase in splitting tensile strength of GFRC after a dosage of 0.5%. He noticed Fiber addition had no significant effect on the modulus of elasticity of BF and GF reinforced concrete. However, the modulus of elasticity of concrete slightly reduced when the dosage of basalt and glass fiber was increased.

Fatigue performances of GFRC concrete in flexure was investigated by Lv et al. (2012). Sixty-three glass fiber reinforced concrete (GFRC) beam specimens of size 100×100×400mm were tested under four- point flexural fatigue loading by the electro-hydraulic universal testing system (MTS) to obtain the fatigue lives of GFRC at various stress levels. The specimens incorporated 0.6%, 0.8% and 1% glass fiber volume fraction. The results indicate that the statistical distribution of fatigue life of GFRC is in agreement with the two-parameter Weibull distribution. The coefficients of the fatigue equation have been determined corresponding to different survival probabilities so as to predict the flexural fatigue strength of GFRC for the desired level of survival probability.

Effects of alkali-resistant glass fiber reinforcement on the flexural strength and ductility, restrained shrinkage cracking and temperature resistance of lightweight concrete were studied by Mirza and Soroushian (2002). All these properties of lightweight concrete benefitted from the introduction of alkali-resistant glass fibers. Fiber mass fractions of 0.5–3.0% (volume fractions of 0.125–0.75%) were investigated; fiber mass fractions of 1.0–2.0% (volume fractions of 0.25–0.5%) were sufficient for control of restrained shrinkage cracks and enhancement of the flexural toughness and temperature resistance of lightweight concrete.

Shah (2009) suggested special methods to reduce the sensitivity to poor and non-uniform water curing. The addition of polymer latex has been reported to be effective in eliminating the adverse effects of lack of water curing. It has been suggested that for AR- GRC, the addition of 5% polymer solids by volume, without any moist curing, may replace the recommended practice of seven days curing in a composite without the polymer.

2.3 Previous Studies on Fiber Reinforced Concrete Corbels

Corbels are structural elements which are built monolithically with columns and its primary function is to support precast members and transfer of vertical and horizontal loads to principle members (column, wall) (Abdul-Razzak and Ali, 2011).

Many experimental and analytical studies were made to determine the strength of such members when subjected to vertical and horizontal forces and to highlighting the role of the parameters that influence the performance of corbels including shape and dimension of corbels, type of main and secondary steel reinforcements, presence and type of fibers, and strength of concrete. It has been widely shown that to increase the strength and improve the ductility of corbels, it is necessary to increase the percentages of transverse steel (generally constituted by horizontal stirrups or inclined bars) or to integrate or partially substitute the secondary shear steel reinforcements by using fiber reinforced concrete (FRC) (Campione, 2007).

Fattuhi (1990) investigated the effect of column load on steel fibers reinforced concrete corbels. The tests were made on concrete corbels reinforced with main bars and steel fibers with the size of 18 150 x 150 x 200 mm. fibers were used as a secondary (shear) reinforcement. A varied shear span to depth ratio was used in the test. A concentric force was applied on the column segment of eight specimens. Test results showed that the corbels failed catastrophically and suddenly after reaching its maximum load when it was reinforced with main bars only. However, the addition of steel fibers to the secondary reinforcement prevented diagonal splitting failure, strength and ductility were improved. The improvement in the latter was more pronounced for corbels reinforced with low percentages of main bars and/or tested at large shear span to depth (a/h) ratios, where an almost elastic-plastic behavior was recorded. The results also

showed that loading the column segment of the specimen or the left-side corbel did not appear to have any significant effect on the load-carrying capacity of the failed (right-side) corbel.

In another study related to SFRC corbels, Fattuhi (1994) studied the strength of FRC corbels in flexure, he concluded that when the fiber volume increased the ductility and strength of corbels were improved. In this study, he proposed that the mode of failure can be changed from shear to flexure by reinforcing corbels with the relatively low volume of main bars.

Kumar (2005) developed an equation to measure the shear strength of corbels reinforced with steel fiber involving a wide range of variables. Kumar presented in his paper analytical investigation on the ultimate shear strength of steel fibrous reinforced concrete corbels without shear reinforcement and tested under vertical loading. The design method consists of idealized strain and stresses distributions at failure and it accounts for the effects of fiber reinforcements on the ductility of shear failure.

Campione (2005) made an analytical and experimental study referring to the flexural behavior of reinforced concrete corbels subjected to vertical forces is presented. For fixed shape and dimensions of the corbels the experimental investigation analyses the effects of the following: longitudinal and transverse steel reinforcements; fiber reinforced concrete (FRC) with hooked steel fibers; external wrapping retrofitting technique with a thin layer of carbon fiber sheet (CFRP). The analytical model proposed is able to determine the bearing capacity of corbels for all cases examined. It is based on the analysis at rupture of corbels by means of equivalent multiple trusses including all the possible modes of failure observed experimentally, such as steel yielding, concrete crushing, external wrap debonding and fiber pull- out. The model shows good agreement with the experimental results and also gives a physical interpretation of the behavior of corbels at rupture.

Campione et al. (2007) studied the flexural behavior of corbels in plain and fibrous concrete and in the presence of steel bars. He proposed a simplified analytical model to estimate the shear strength of FRC concrete corbels. The result showed the effectiveness of adding fibers to concrete which was clear in improving the strength and deformation capacity in fibrous reinforced concrete corbels.

Campione (2009) proposed a softened strut-and-tie macro model which predict the flexural behavior of corbels in plain and reinforced fibrous concrete, including softening of compressed struts and yielding of main and secondary steel bars, is presented in this paper. The proposed model was subjected to horizontal and vertical forces. The load deflection curve was determined with varied types of concrete (normal and high strength) and different fibers ratios were used.

The results of his study showed that addition of fibers to the corbels improved the concrete significantly in terms of strength and ductility. Fibers were used to reduce the brittleness of concrete which can be an excellent alternative to transverse stirrups.

Yang et al. (2008) studied the mechanical response of high strength steel fiber reinforced concrete corbels by the use of a different amount of fibers and two anchorage types (welding to transverse bar and headed). They proved that usage of steel fibers improve important mechanical properties (load carrying capacity, stiffness, ductility and crack width) of high strength corbels. They also proved that headed bars anchorage type gives better results about load carrying capacities and ductility of high strength SFRC corbels as compared to welding to transverse bar anchorage type.

Kumar and Barai (2010) developed an artificial neural network (ANN) model is presented to measure the ultimate shear strength of steel fibrous reinforced concrete (SFRC) corbels without shear reinforcement and tested under vertical loading. The model gave satisfactory predictions of the ultimate shear strength when compared with test results and some existing models.

Abdul-Razzak and Ali (2011) presented new constitutive models for high strength steel fiber reinforced concrete. Their study was based on the experimental data from the literature. The models were developed gave good results for the analysis of high strength steel fiber reinforced concrete corbels subjected to the incremental loading up to failure.

A macro-mechanical strut and tie model is proposed for the analysis of fibrous high-strength concrete corbels by Khalifa (2012). In the proposed model the horizontal stirrups can be replaced by fibers. The effect of fiber volume, fiber length, and fiber diameter, random distribution of fibers, fiber HSC interface and shear span-to-depth ratio were taken into consideration in the analytical macro-mechanical model. The

model was compared with experimental results found in literature and a good agreement is obtained.

2.4 Approaches for Corbel Design

2.4.1 ACI Code provisions for corbel design

The ACI Code 16.5 introduced design provisions for brackets and corbels which mainly based on studies made by Mattock et al. (1975), Kriz and Raths (1965) and Elzanaty et al. (1986). These provisions should be applied on corbels with a_v/d 1.0 or less (see Fig. 2.1). Brackets and corbels with a_v/d ratio more than unity can be designed using strut and tie models.

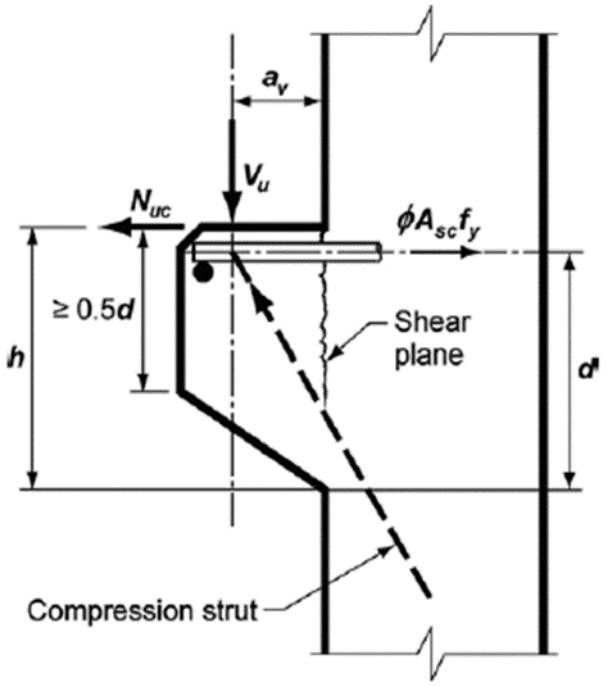

Figure 2.1 Structural action of corbel (ACI 318-14, 2014)

As it's shown in the figure the corbel may fail along the column corbel interface which it is a shear failure or it may fail by yielding the main reinforcement or it can fail due to the splitting of the compression strut and it may fail because of localized bearing end failure.

The effective depth d is measured at the column face, and the minimum depth at the outside edge of the bearing area should be 0.5d.

The section should be designed to resist the shear V_u, the horizontal force N_{uc} and the moment $M_u = V_u a_v + N_{uc} (h — d)$. Unless the tensile force prevented from acting on the corbel, a horizontal tension will be at least 0.2 V_u. This tensile force N_{uc} is shall be treated as a live load.

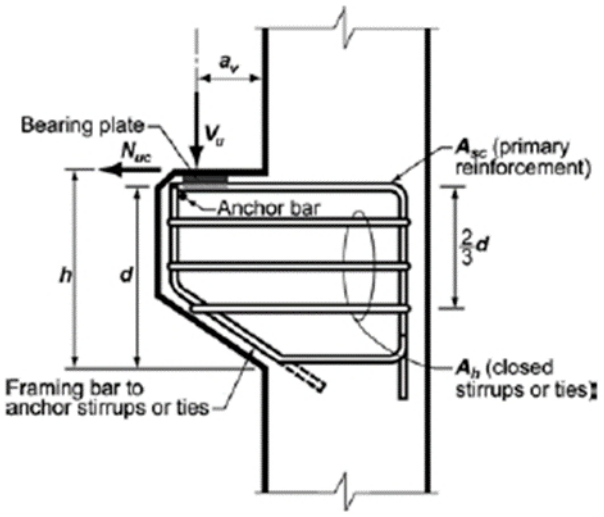

Figure 2.2 Typical reinforced corbels with loads and reinforcements (ACI 318-14, 2014)

The design must satisfy $\phi N_n \geq N_{uc}$, $\phi V_n \geq V_u$ and $\phi M_n \geq M_u$ where ϕ is equal 0.75 according to section 21.2 of ACI Code.

The nominal tensile strength N_n can be determined by:

$$N_n = f_y A_n \tag{2.1}$$

Where

N_n: the nominal tensile strength.

f_y: yield stress of the reinforcement.

A_n: extra main steel provided for horizontal loads.

The ACI code proposed the nominal shear strength V_n will be determined by shear friction equation

$$V_n = f_y A_{vf} \mu \tag{2.2}$$

Where

V_n: Nominal shear design strength.

A_{vf}: Area of reinforcement that crosses that assumed shear plane.

f_y: Yield stress of reinforcement.

μ: The coefficient of friction.

An amount of steel reinforcement A_f is needed to resist the moment M_u can be calculated by:

$$A_f = \frac{M_u}{\phi f_y \left(d - \frac{a}{2} \right)} \tag{2.3}$$

Where

$$a = \frac{A_f f_y}{0.85 f_c'} \tag{2.4}$$

According to ACI code the primary tension reinforcement area A_{sc} should be the greatest of:

$$A_f + A_n, \frac{2}{3} A_{vf} + A_n, 0.04 \left(\frac{f_c}{f_y} \right) (b_w d) \tag{2.5}$$

According to the ACI Code, closed hoop stirrups having area A_h (see Fig. 2.2) not less than 0.5(*Asc* - *An*) must be provided and be uniformly distributed within two-thirds of the effective depth measured from the primary tension reinforcement.

2.4.2 Previous studies on corbel design

Kriz and Raths (1965) presented an empirical formula to estimate the strength of corbels based on the experimental study, A 195 corbel were used in the investigation out of which 124 loaded with a vertical load only, and 71 subjected to vertical and horizontal load. Varied parameters were included in their study, as result an equation to calculate the ultimate design load capacity for corbels were proposed:

$$V_u = \phi \left[6.5 b d \sqrt{f_c'} \left(1 - 0.5^{\frac{d}{a}} \right) \frac{1000 \rho^{\left(\frac{1}{3} + 0.4 \frac{H}{V} \right)}}{10^{0.8 \frac{H}{V}}} \right] \tag{2.6}$$

V_u: Vertical load at ultimate strength, i.e. shear at ultimate strength, lb

∅: Capacity reduction factor

H/V: Ratio of horizontal load to vertical load

a: Shear span, in.

b: Width of corbel, in.

d: Effective depth of the corbel, in.

f_C: Concrete cylinder strength, psi.

ρ: Reinforcement ratio.

The equation has been simplified to avoid complexity into this form:

For vertical load only:

$$V_u = \phi bd\sqrt{f_c'}F_1F_2 \tag{2.7}$$

For vertical and horizontal loads:

$$V_u = \phi bd\sqrt{f_c'}F_1F_3 \tag{2.8}$$

Where

$$F_1 = 6.5\left(1 - 0.5\tfrac{d}{a}\right) \tag{2.9}$$

$$F_2 = (1000\rho)^{\frac{1}{3}} \tag{2.10}$$

$$F_3 = \frac{(1000\rho)^{\left(\frac{1}{3}+0.4\frac{H}{V}\right)}}{10^{0.8\frac{H}{V}}} \tag{2.11}$$

Values of F1, F2 and F3 are empirical parameter values dependent on the shear span-depth ratio, reinforcement ratio, and the ratio of horizontal to vertical load. For fast calculations these values of F1, F2 and F3 are tabulated as shown in Table 2.1. At the same time, the design method is interpreted in the format of design charts for quick and simple design procedures as shown in Fig. 2.3.

Table 2.1 Values of F1, F2, and F3 based on Kriz and Raths (1965) results

Value of $F_1 = 6.5\left(1 - 0.5\frac{d}{a}\right)$										
a/d	*0.00*	*0.01*	*0.02*	*0.03*	*0.04*	*0.05*	*0.06*	*0.07*	*0.08*	*0.09*
0.0	*6.50*	*6.50*	*6.50*	*6.50*	*6.50*	*6.50*	*6.50*	*6.50*	*6.50*	*6.50*
0.1	*6.49*	*6.49*	*6.48*	*6.47*	*6.45*	*6.44*	*6.41*	*6.39*	*6.36*	*6.33*
0.2	*6.30*	*6.26*	*6.22*	*6.18*	*6.14*	*6.09*	*6.05*	*6.00*	*5.95*	*5.90*
0.3	*5.85*	*5.80*	*5.75*	*5.70*	*5.65*	*5.60*	*5.55*	*5.50*	*5.45*	*5.40*
0.4	*5.35*	*5.30*	*5.25*	*5.20*	*5.15*	*5.10*	*5.06*	*5.01*	*4.97*	*4.92*

0.5	4.87	4.83	4.79	4.74	4.70	4.66	4.61	4.57	4.53	4.49
0.6	4.45	4.41	4.37	4.34	4.30	4.26	4.22	4.19	4.15	4.12
0.7	4.08	4.05	4.02	3.98	3.95	3.92	3.89	3.86	3.83	3.80
0.8	3.77	3.74	3.71	3.68	3.65	3.62	3.60	3.57	3.54	3.52
0.9	3.49	3.46	3.44	3.42	3.39	3.37	3.34	3.32	3.30	3.27

Value of $F_2 = (1000\rho)^{\frac{1}{3}}$

ρ	F2	ρ	F2	ρ	F2
0.0040	1.59	0.0095	2.12	0.0150	2.47
0.0045	1.65	0.0100	2.15	0.0155	2.49
0.0050	1.71	0.0105	2.19	0.0160	2.52
0.0055	1.76	0.0110	2.22	0.0165	2.54
0.0060	1.82	0.0115	2.26	0.0170	2.57
0.0065	1.87	0.0120	2.29	0.0175	2.60
0.0070	1.91	0.0125	2.32	0.0180	2.62
0.0075	1.96	0.0130	2.35	0.0185	2.64
0.0080	2.00	0.0135	2.38	0.0190	2.67
0.0085	2.04	0.0140	2.41	0.0195	2.69
0.0090	2.08	0.0145	2.44	0.0200	2.71

Value of $F_3 = \dfrac{(1000\rho)^{\left(\frac{1}{3}+0.4\frac{H}{V}\right)}}{10^{0.8\frac{H}{V}}}$

H/V												
ρ	0.1	0.2	0.3	0.4	0.5	0.6	0.7	0.8	0.9	1.0	1.1	1.2
0.0040	1.40	1.23	1.08	0.95	0.83	0.73	0.64	0.57	0.50	0.44	0.38	0.34
0.0045	1.46	1.29	1.14	1.00	0.89	0.78	0.69	0.61	0.54	0.48	0.42	0.37
0.0050	1.52	1.34	1.19	1.06	0.94	0.83	0.74	0.66	0.58	0.52	0.46	0.40
0.0055	1.57	1.40	1.25	1.11	0.99	0.88	0.78	0.70	0.62	0.55	0.49	0.44
0.0060	1.62	1.45	1.30	1.16	1.04	0.92	0.83	0.74	0.66	0.59	0.53	0.47
0.0065	1.67	1.50	1.34	1.20	1.08	0.97	0.87	0.78	0.70	0.62	0.56	0.50
0.0070	1.72	1.55	1.39	1.25	1.12	1.01	0.91	0.82	0.73	0.66	0.59	0.53
0.0075	1.76	1.59	1.43	1.29	1.16	1.05	0.95	0.85	0.77	0.69	0.63	0.56
0.0080	1.81	1.63	1.48	1.34	1.21	1.09	0.99	0.89	0.80	0.73	0.66	0.59
0.0085	1.85	1.68	1.52	1.38	1.25	1.13	1.02	0.93	0.84	0.76	0.69	0.62
0.0090	1.89	1.72	1.56	1.41	1.28	1.17	1.06	0.96	0.87	0.79	0.72	0.65
0.0095	1.93	1.75	1.60	1.45	1.32	1.20	1.10	1.00	0.91	0.83	0.75	0.68
0.0100	1.96	1.79	1.63	1.49	1.36	1.24	1.13	1.03	0.94	0.86	0.78	0.71
0.0105	2.00	1.83	1.67	1.53	1.40	1.27	1.16	1.06	0.97	0.89	0.81	0.74
0.0110	2.04	1.86	1.71	1.56	1.43	1.31	1.20	1.10	1.00	0.92	0.84	0.77
0.0115	2.07	1.90	1.74	1.60	1.46	1.34	1.23	1.13	1.04	0.96	0.87	0.80
0.0120	2.10	1.93	1.78	1.63	1.50	1.38	1.26	1.16	1.07	0.98	0.90	0.83
0.0125	2.14	1.96	1.81	1.66	1.53	1.41	1.30	1.19	1.10	1.01	0.93	0.86
0.0130	2.17	2.00	1.84	1.70	1.56	1.44	1.33	1.22	1.13	1.04	0.96	0.88

The design procedures include the following limitations:

1. The presented formula in the equation 2.6 can be applied on corbels with a/d ≤ 1.
2. The least amount of tension reinforcement As *is 0.004bd.*
3. Welding a cross bar to the ends of the tension reinforcing bar should be used for anchoring the main tension reinforcement. The minimum crossbar size must be equal to the maximum size for a bar used as tension reinforcement.
4. Closed horizontal stirrups have to be provided total area not less than 50% of the area of the main tension tie reinforcement. The distribution of these stirrups should be throughout the upper two-thirds of the effective depth of the face of the column.
5. The outside edge of the bearing plate should be at least equal to 2 inches from the outer face of the corbel.
6. Steel bearing plates should be welded to the tension reinforcement to transfer the horizontal forces to the tension reinforcement.
7. Bearing stresses at ultimate load should not be more than $0.5f_{\acute{c}}$.

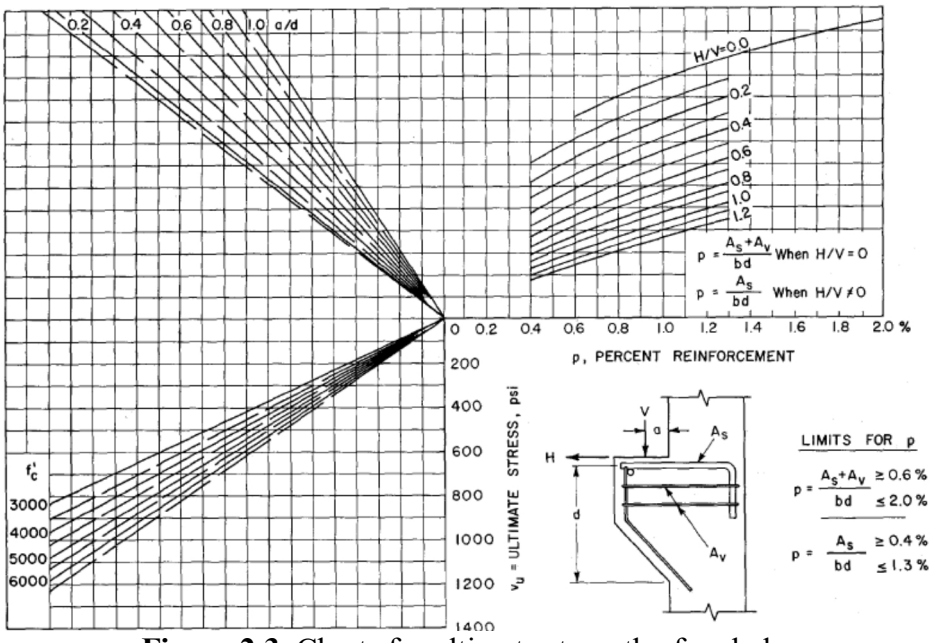

Figure 2.3 Charts for ultimate strength of corbels

Franz and Niedenhoff (1963) in their research corbels were treated as truss under a triangle of forces as it illustrated in Fig. 2.4:

Based on their experiments they concluded the following:

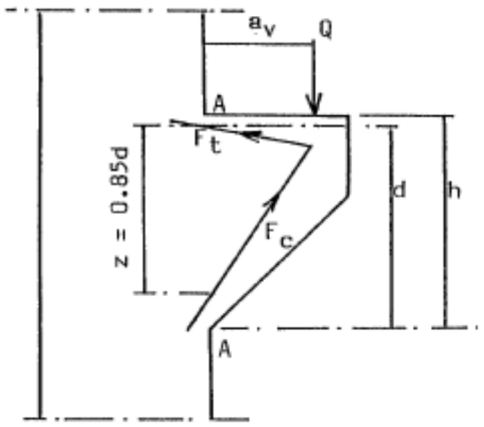

Figure 2.4 Truss analogy suggested by Franz and Niedenhoff (1963) for designing concrete corbels

1. The state of stresses will not be affected by the shape of corbels whether rectangular or trapezoidal.
2. The tensile stress is almost constant at the upper region of corbel between the bearing area and the column face.
3. The stresses are almost zero at the outer-bottom comer of a rectangular corbel.

Regarding the crack patterns and final failure of corbels, Franz and Niedenhoff have claimed that the crack pattern largely agrees with the pattern of stress trajectories irrespective of the arrangement of reinforcement. They made the following recommendations for design:-

1. Reinforcement should be provided in the compression zone of the corbel.
2. Horizontal or inclined web reinforcement should not be less than 0.25Ast (Ast = main tensile reinforcement).
3. Main reinforcement should be placed horizontally and must be well anchored at both ends by bending the bars into closed loops, or by other means to provide full anchorage.
4. At the face of the column, the column reinforcement should be increased by local bars and extended a certain distance to resist the increase in tensile force above the bracket around the column.
5. It is necessary to reinforce the compressive face of the corbel - with at least 6-14mm bars per meter width to enhance resistance against buckling.

Mast (1968) presented the shear friction theory in his approach, Mast's objective was to develop a design technique for different types of concrete connections based on the

behavior of physical models rather than on an empirical basis. The new technique has been applied to the design of interface connections in composite beams. Then he extended it to corbels using Kriz and Rath results. He considered only those specimens where steel had yielded and with a shear span-depth ratio less than 0.7.

Mast proposed that concrete may crack and failure occurs in an undesirable manner with which to prevent such failure a reinforcement should be provided. In practice, this crack might never take place and the concrete specimen will be much stronger than the design calculations would indicate. Mast's philosophy is that the crack might occur and the possibility of the crack occurring should be guarded against. Mast considered this philosophy to be applicable to the design of all concrete connections.

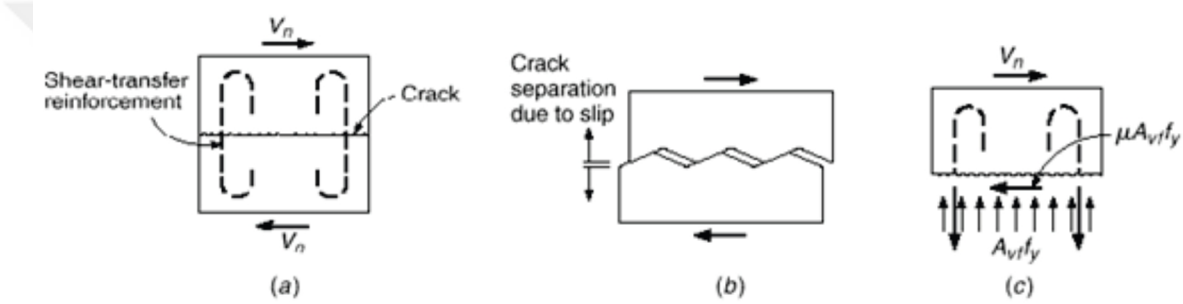

Figure 2.5 Basis of Shear-Friction Design Method: a) Applied Shear; b) Enlarged Representation of Crack Surface; c) Free-Body Sketch of Concrete above Crack. (Nilson et al, 2004)

The shear friction concept states that at the interfaces of a cracked concrete section a shear resistance is provided by aggregate interlock. This shear resistance at the interface is balanced in turn by the reinforcement, hence allowing it to yield. Mast proposed that this horizontal shear resistance force, *Vn,* could be obtained by multiplying the vertical force *Avfh* by the angle of internal friction (also referred to as coefficient of friction), μ*;* which transforms the vertical force to a horizontal shear resistance. Mast assumes the following:

1. Reinforcement crossing cracks are sufficiently anchored and can develop their full yield strength.
2. The cohesive strength of concrete can be ignored.

3. The values of the coefficient of friction, μ; are determined from tests and are independent of the strength of concrete and stress level.

Cook and Mitchell (1988) developed nonlinear finite element program (FIELDS) that is capable of predicting complete responses of corbels (see Fig. 2.6), FIELDS was used to study the flow of internal forces in "disturbed regions" as in corbels, beams, beams with openings, dapped end beams and deep beams have been studied.

Cook and Mitchell have compared the results from two approaches, using the simple strut and tie model and their finite element computer program.

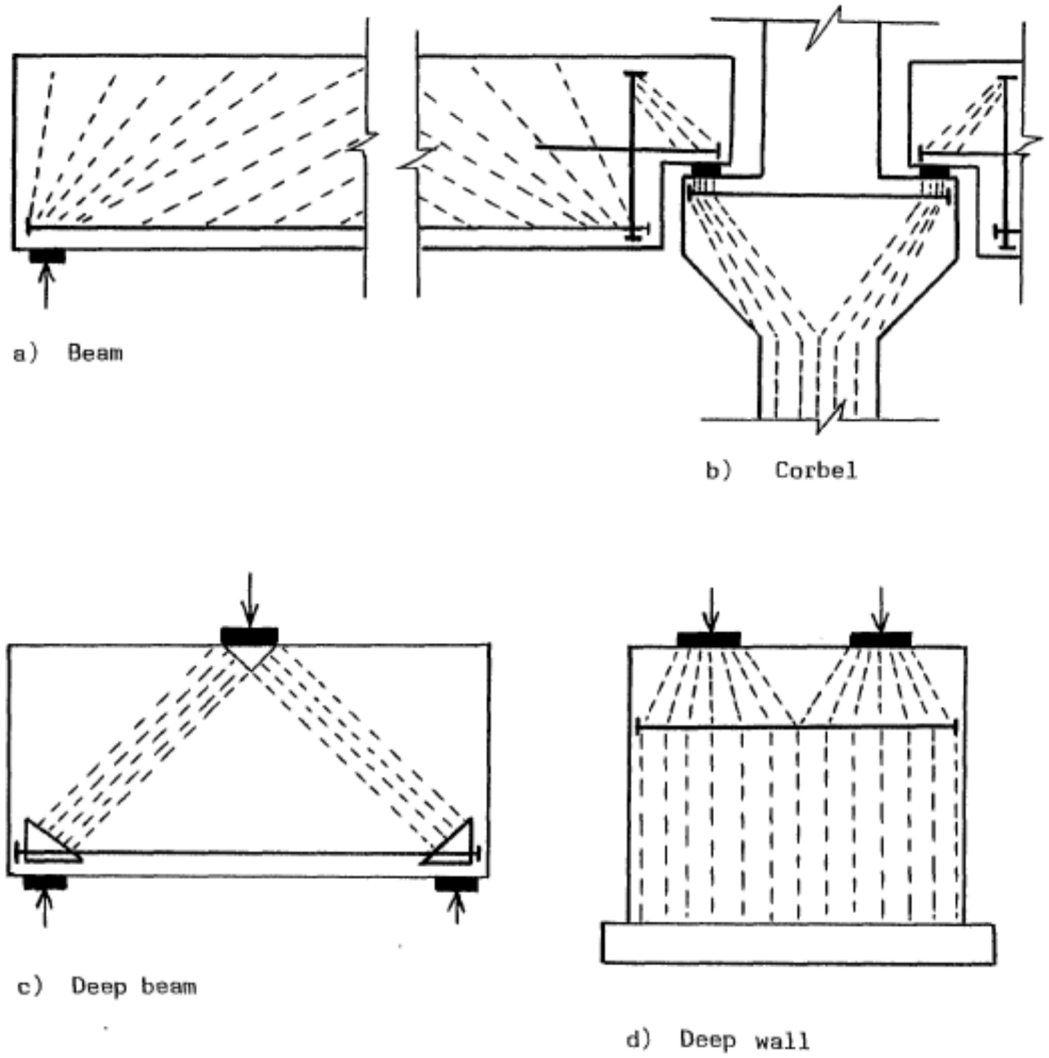

Figure 2.6 Distributed regions and force flowing (Cook and Mitchell, 1988)

Siao (1994) described a method for analyzing the shear strength of short shear-walls with height to length ratio of unity or less, top-loaded deep beams and corbels. A compression strut is present in all three elements, where shear force is transmitted to the support via a strut-and-tie system. By using the refined strut-and-tie system, shown in Fig. 2.7.

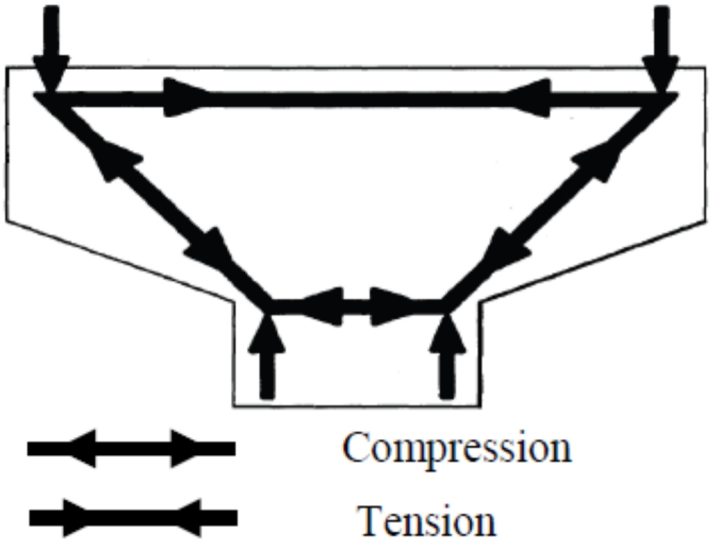

Figure 2.7 Refined strut and tie model (Siao, 2004).

The ultimate shear capacity may be calculated as follows:

$$V_u = 1.8 f_t bd \tag{2.12}$$

Where:

f_t: Allowable tensile strength of tension tie in refined compression strut which is calculated prior to crack, and after cracking.

$$f_t = 7\sqrt{f_c'}\left[1 + n\left(\rho_{h\cdot} \cdot \sin^2\theta + \rho_v \cdot \cos^2\theta\right)\right] \tag{2.13}$$

$$f_t = f_y\left(\rho_{h\cdot} \cdot \sin^2\theta + \rho_v \cdot \cos^2\theta\right) \tag{2.14}$$

Where:

f_y: Steel yield strength.

n: Ratio of the elastic modulus of steel and concrete.

ρ_h: Steel reinforcement ratio of horizontal bars.

ρ_v: Steel reinforcement ratio of vertical bars.

θ: Inclination of compression strut to tension tie.

Aziz (2001), studied the effect of crushed stone and their contribution to the shear strength of reinforced concrete corbels. 11 specimens were cast for this purpose, having the same dimensions, the variables studied were the type of aggregate used (normal gravel or crushed stones), the amount of longitudinal reinforcement, the amount of shear reinforcement, the compressive strength of concrete and the shear span to depth ratio, (*av/d*). The researcher found that for the same proportion, workability curing, and testing conditions, the crushed stone concrete shows higher values of compressive strength, tensile strength, shear stress when compared with the natural gravel concrete. The shear stress was increased with the increasing of the amount of longitudinal, Shear reinforcement and compressive strength of concrete, and it was decreased with the increasing of the shear span to depth ratio (*av/d*).

According to the results obtained from this test and other results of 168 reinforced concrete corbels failing in shear, taken from literature, an equation for shear was proposed as follows:

$$V_u = 2.38\left(\frac{f_c'\frac{k}{d}(\rho_h + \rho_w)}{\frac{a}{d}}\right)^{0.175} \qquad (2.15)$$

Where:

V_u: Ultimate shear stress of reinforced concrete corbels, N/mm^2.

f_c: Compressive strength of concrete, N/mm^2.

K,d: Properties of the section,

a/d: Shear span to depth ratio.

ρ_h,ρ_w: Longitudinal and shear reinforcement ratios.

2.5 Modes of Failure in Corbels

Kriz and Rath (1965) suggested five possible types of failure that may take place in corbels. These five modes are summarized below:-

1. Flexural tension failure

This mode of failure involves the yielding of the tension reinforcement which is desirable since it is a ductile failure that allows a force redistribution to take place easily. It is characterized by a very wide flexural crack at the junction of the column and the corbel. Further, this mode occurs in corbels with bigger shear span-depth ratio and concrete is crushed at the bottom (compression zone) after extensive yielding of tension reinforcement.

2. Flexural compression failure

The corbel usually remains stable after the formation of the first crack in flexure. Further increase in the load causes the diagonal crack which starts at the inner edge of the bearing support plate and propagates into the compression zone until failure of concrete finally occurs in the compression zone.

The concrete crushing failure takes place before yielding of the tension reinforcement occurs. Compression failure happens suddenly and often explosively. Corbels fail in this manner without plastic deformation of steel. This mode of failure is observed with over-reinforced concrete corbels.

3. Diagonal crack or tension failure

This occurs in corbels where large tensile stresses are produced in concrete across the diagonal joining the support and the load point as explained more fully in later sections. Also, this crack is developed in corbels as a result of the sudden transfer of stresses from the reinforcement to the concrete, due to the fact that concrete can only take limited stresses before it cracks and becomes stress-free. Soon after the tensile stress exceeds the tensile strength of the concrete it splits. This type of failure occurs at relatively smaller a/d ratios than those at which flexural tension failure occurs.

4. Shear failure

This type of failure is observed as short inclined cracks formed along the plane of the interface between the column and the corbel. Failure of the corbel will then be due to shearing along this weakened plane.

5. Secondary Modes of Failure

Failures which did not involve the deepest section of the corbel at the column face were considered. Secondary modes of failure. These were of two types:

(1) The splitting away of a portion of the concrete due to a major crack intersecting the sloping face of the corbel.

(2) Bearing failures of the concrete beneath the bearing plate. Both types of secondary modes of failure occurred at loads lower than those at which failure would have occurred by one of the principal modes.

CHAPTER 3

EXPERIMENTAL PROGRAM

3.1 Introduction

This chapter presents the experimental investigation about high strength concrete corbels reinforced with glass fibers. The aim of the study was to observe the behavior of high strength concrete corbels with and without the glass fiber.

A total of 9 corbels were made, the corbels were divided into three groups with various parameters. Different percentage of glass fibers 0%, 0.2% and 0.4% were used with three shear spans used in the test (8, 10, and 12) cm. All the corbels were reinforced with 2×ϕ8mm steel reinforcement bars.

Additional tests were made on concrete cylinders and cubes to establish the compressive and tensile strengths of the concrete used in fabricating the corbels. The results of the experiments will be explained in Chapter 4.

3.2 Description of Test Specimen

Nine double sided corbels were made and tested in the mechanical laboratory at Gaziantep University. All the corbels had the same dimensions and reinforcements details. The width of corbels is 150 mm. both of column have the same cross section (150 × 150) mm. the stubs of the column extended by 160 mm from above and 100 mm from below. Fig. 3.1 illustrates the dimensions of the corbel.

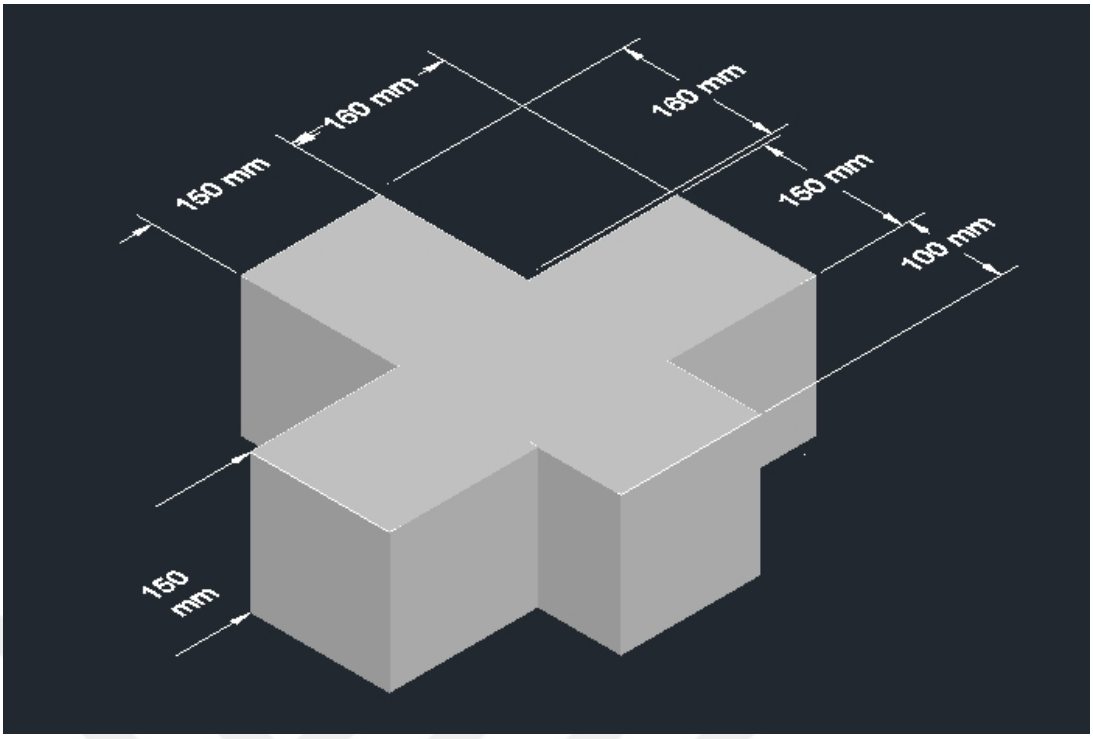

Figure 3.1 Dimensions of the corbel

The column was reinforced with four vertical bars ϕ12mm in diameter and 4 stirrup reinforcement were provided in the form of closed ties at a spacing of 90 mm. The main tension reinforcement of the corbel consisted of two (8mm Diameter) steel bars. Fig. 3.2 shows the details of the reinforcements.

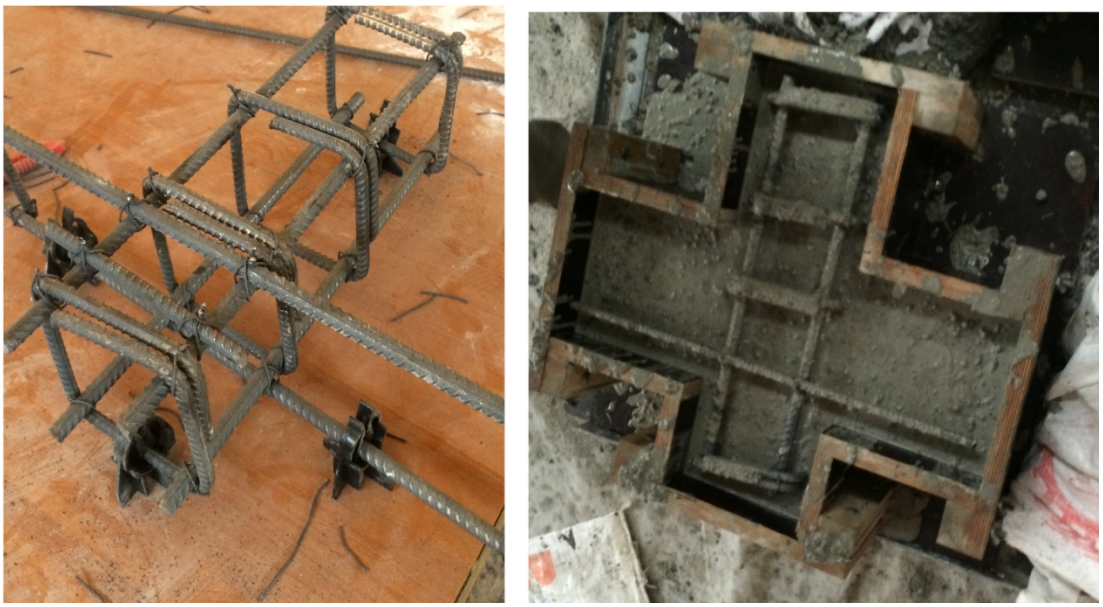

Figure 3.2 Reinforcement of the specimen

3.3 Mix Design and Material Properties

High strength concrete was used. The cement used in all concrete mixes was 32.5R Portland. Coarse aggregate (crushed stone nominal maximum size of 10 mm), fine aggregate size interval 0-5, fly ash chemical class "F" particle density 2350 ± 200 meeting the requirements of "TS EN 450-1". Properties of the glass fiber are shown in Table 3.1.

Table 3.1 Properties of the glass fiber

Diameter (micron)	13
Specific weight (g/cm3)	2.6
Modulus (GPa)	77
Tensile strength (MPa)	3400
Length (mm)	13

Average yield strengths for reinforcements were found to be 550 MPa and 486 MPa, and average ultimate strength values found to be 640 MPa and 624 MPa, between 8 mm and 12 mm steel bars, respectively.

Concrete mix proportion used in the experimental program is shown in table 3.2 for high strength concrete. Hence adding fibers can reduce the workability of the concrete mix, thus, the dosage of water was increased to reach 0.37 for the concretes containing fibers to maintain the workability of the concrete.

Table 3.2 Concrete mix proportion of 1 m^3 concrete

Material	weights
Course aggregate (kg)	670
Fine aggregate (kg)	1000
Cement (kg)	450
Fly ash (kg)	50
Silica fume (kg)	35
Water (kg)	150
Viscocrete (kg)	6.42
w/c ratio	0.33

3.4 Preparation of the Specimens

The concrete was mixed in 150 liters capacity vertical mixer. Coarse, fine aggregate and cement were dry-mixed for 30 seconds. This was followed by the addition of fly ash, silica fume, fiber and water, and the viscocrete, with a mixing time of 5-10 min. Corbels were cast in a horizontal position, the concrete was placed in layers and each layer was compacted by means of a vibrating table, to prevent air voids inside the concrete and to place the concrete into the formwork effectively. During the casting, extra care was given to prevent bleeding and segregation around the steel bars on the formwork surface. Before the concreting process, all of the corbel formworks and sample formworks were lubricated by special formwork grease. With each batch three specimens were prepared, three batches were made of concrete contain 0%, 0.2% and 0.4% of glass fiber.

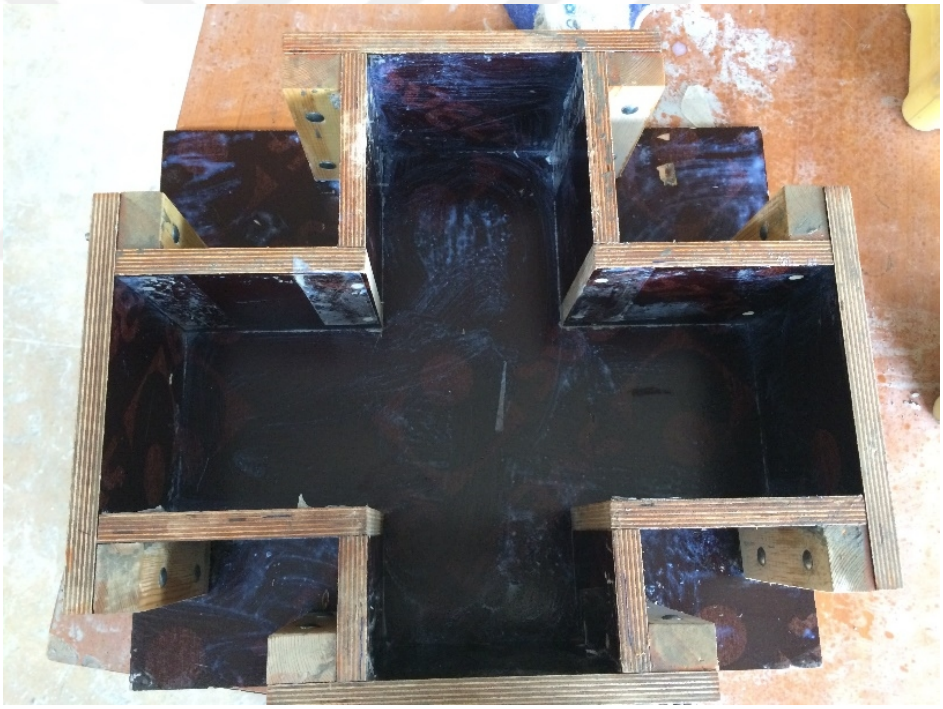

Figure 3.3 Oiled molds before casting

Figure 3.4 Concrete patch

Six cylinder samples (10mm × 20mm) and three cube samples (10mm × 10mm) were prepared with every concrete batch see fig 3.5. Three of the cylinders were used to evaluate compressive strength of the concrete, while the other three were used to measure the splitting tensile strength of the concrete. Three cubes were made to evaluate the cubic compressive strength of the concrete.

Figure 3.5 Casting of cylinders and cubes

The specimens were demolded after 1 day of casting and then placed in a curing tanks in a room with 90% relative humidity and 23 C for 21 days of curing. For 7 days prior to the tests, the specimens were allowed to air dry in the laboratory.

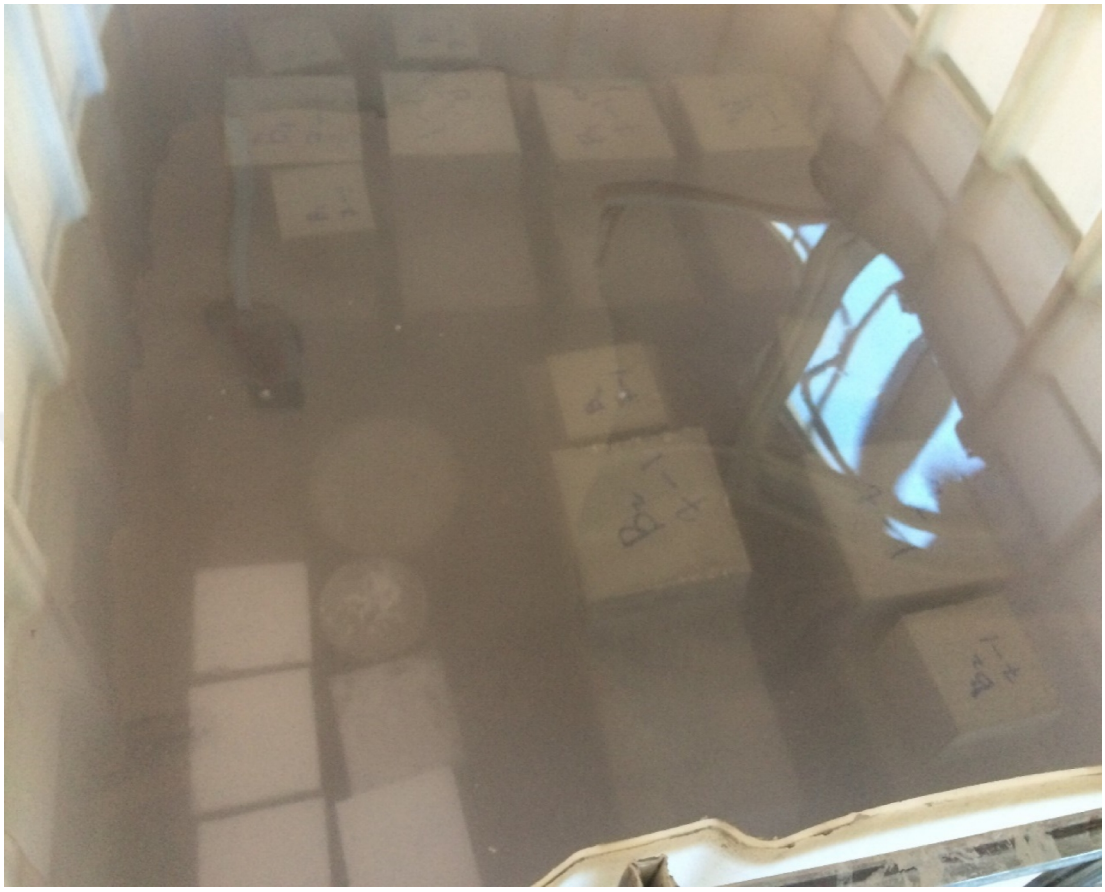

Figure 3.6 Curing of specimens

3.5 Setup and Testing Procedure of the Specimens

A testing machine with a bearing capacity of 500 KN was used to perform flexural tests and the load was applied at the top of the column. The machine operated in a controlled displacement mode with rate of displacement of 0.2 mm/minute. The load scheme adopted is shown in Fig 3.7. Corbels were supported symmetrically by a steel hinge and roller. Three different spans 80mm, 100mm, 120mm were used for each group of corbels.

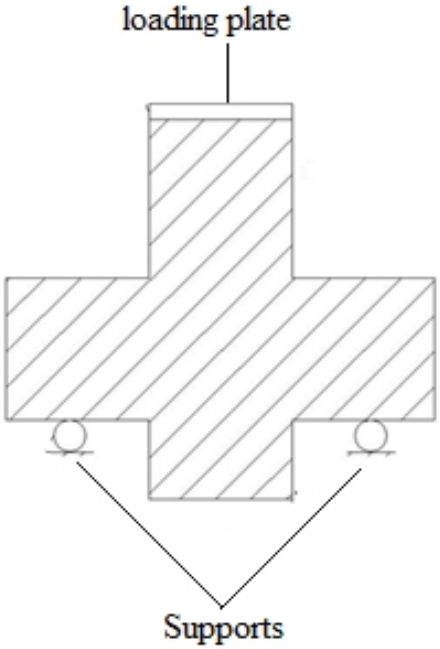

Figure 3.7 Setup of corbel in the testing machine

The load was transferred from the loading frame to the corbel by the 15 mm thickness loading plate. Loading plate was produced from a transmission steel to transfer the load effectively and continuously until failure. Photographs of cracks and crack patterns were taken at each load stage. Two dial gauges were used to measure the deflection. The loads and the readings of the dial gauges were taken manually after every 0.2 mm. Therefore, the behavior of corbels could be followed and load-displacement curve could be drawn. After general yielding of the test specimen, the loading stages were taken at 0.3-0.5 mm displacement increments of the head of the testing machine. The testing continued until failure of the specimens.

This test enabled to determine three important values: the ultimate bearing capacity of the corbel, load-strain curve, and it showed failure mode of the corbel subjected to a vertical load.

Compressive strength tests were carried out in accordance with ASTM C 39. Three cylinders and three cubes of GFRC, and plain high strength concrete at 28 days were tested. The load was applied at a rate of 0.02 mm/s. The peak load was recorded during the test by an acquisition system. Compression test set-up used in this study is shown in Fig. 3.8.

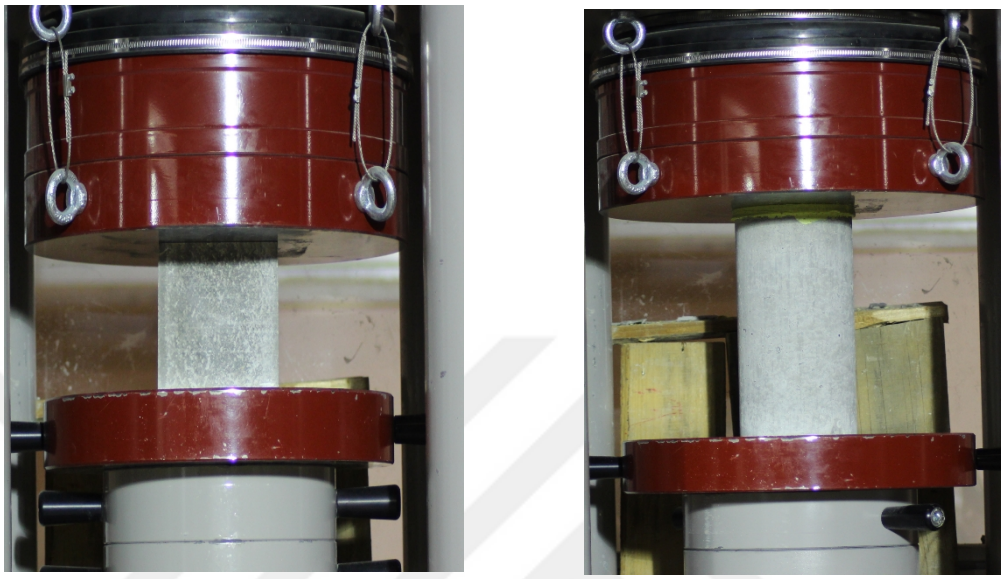

Figure 3.8 Compression test of cubes and cylinders

The split tensile test was carried out in accordance with ASTM C-496 standards on three cylinders of each patch at the same age of specimens of concrete used for the compression test. A typical split-cylinder test set-up used in this study is shown in Fig 3.9.

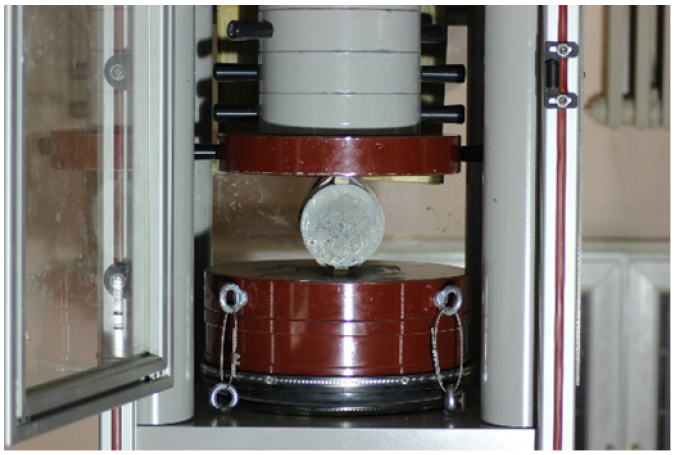

Figure 3.9 Splitting tensile test

The split tensile test is relatively simple and seems to provide a reliable test result to calculate the tensile strength of concrete under uniform stresses at the top and bottom across the diameter of the tested cylinder specimens. Therefore, the split-tensile test is preferred in this investigation. Each cylinder specimen was placed on its side and loaded in compression along a diameter of the specimen. The load was applied at a rate of 0.01 mm/s for the split tensile test. The splitting tensile strength, f_{st} (MPa), was calculated using the following equation:

$$f_{st} = \frac{2P}{\pi LD} \tag{3.1}$$

Where:

P: is the peak load in the test.

L: is the length of the cylinder specimen.

D: is the diameter of the cylinder specimen.

The average compressive and splitting tensile strength of GFRC and plain concrete at 28 days are given in Table 3.3.

Table 3.3 Experimental compressive and splitting tensile strength

	High strength concrete			
Sample no:	GF ratio	f_c (MPa)		f_{st} (MPa)
		Cube	cylinder	
1	0.0	102.66	92.79	4.79
2	0.2%	96.15	83.76	4.99
3	0.4%	98.69	88.26	5.14

Prior to the compression tests, sulfur cabbing was made to the cylinders. To ensure that the specimen has smooth, parallel, uniform bearing surface that is perpendicular to the applied axial load during compressive testing. ASTM C39 require flat the ends of compressive test specimens be plane to within 0.002 inches (0.05 mm) and that the deviation of end faces from being perpendicular to the specimen axis is less than 0.5°. Fig. 3.10 shows the capping of cylinder specimen before the compressive test.

Figure 3.10 Sulfur capped specimen

CHAPTER 4

RESULTS AND DISCUSSION

4.1 Introduction

Concrete is the most widely used construction material, present and past. Recent improvements in the quality of essential materials such as cement, coarse and fine aggregate in addition to the encouragement of using superplasticizer in conjunction with efficient techniques have made it possible to achieve high strength concrete in excess of 100 N/mm^2 at 28 days.

The major difference between the normal strength concrete and high strength concrete is that the high strength concrete tends to behave as an elastic and more brittle material compared with normal strength concrete.

Further, the concrete of up to 120 N/mm^2 has been used in high rise building in Seattle, USA (Godfrey, 1987). The primary advantages of using high strength concrete in columns have made it possible to reduce the column size. As a result, a direct saving on cost could be achieved from the reduction in self-weight and the reduction of other structural components. With the general trend of using high strength concrete in columns, and since most precast columns have corbels, therefore, high strength concrete corbels are becoming more and more important. However, for design purposes, knowledge of the overall structural behavior of high strength concrete corbels reinforced with glass fiber under load and the mechanism of failure is essential. An experimental investigation on high strength concrete corbels, with various glass fiber ratios and at different shear span/depth ratios, this chapter presents the responses of each test specimen. The load-deflection responses, the ultimate bearing capacity, and the crack response.

4.2 Response of Specimen (S8-80)

Specimen (S8-80) is a corbel specimen reinforced with ϕ8 mm steel bars for the main reinforcement of the beam, cast without fiber and subjected to vertical loads with a shear span equal to 80 mm. This specimen used as a comparison specimen to examine the load bearing capacity of the corbels and cracking patterns of high strength corbels with different ratios of glass fibers.

Fig. 4.1 shows the load-displacement response of this test specimen. The first hairline crack observed on the east side of the beam of corbel at load, 67 kN. This crack followed by another crack on the west side at a load of 83 kN, (see Fig. 4.2), those cracks grown and extended. At a load of 201 kN, failure occurred in an explosive manner by a diagonal shear crack on the east side of the specimen, (see Fig.4.3). The displacement of the center (near the inner edges of the corbel) was 1.75 mm. The key load stages and the details of the corbel are shown in Table 4.1.

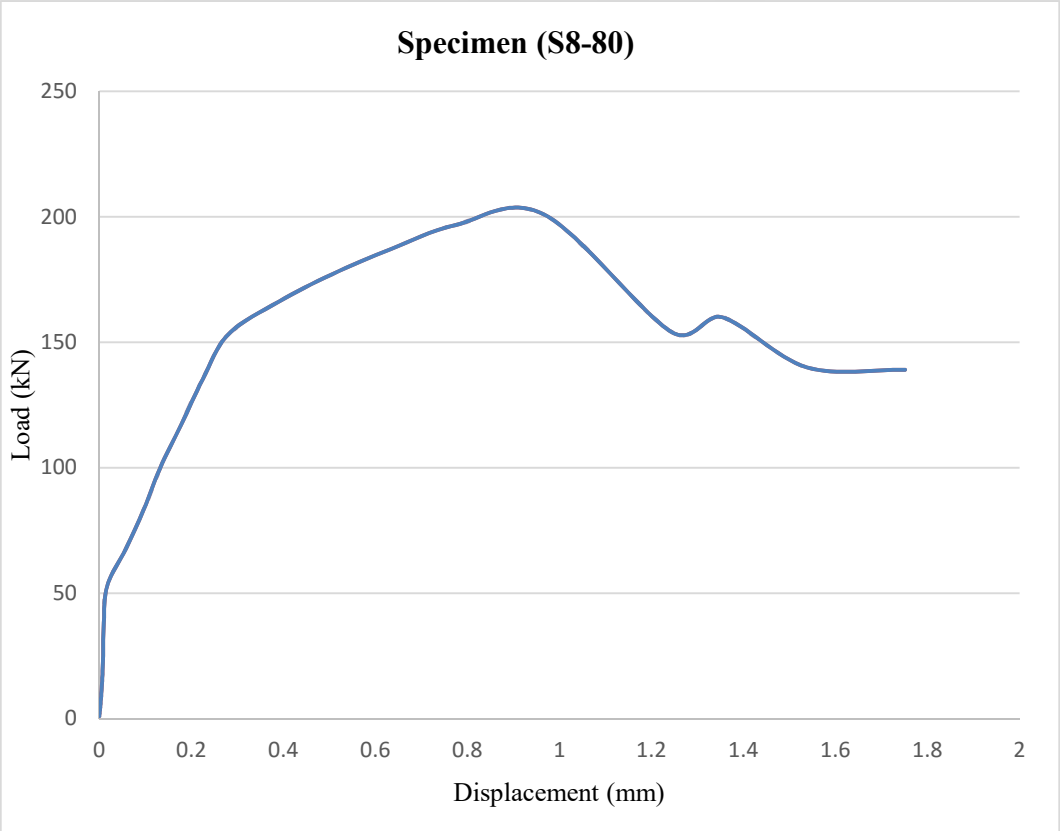

Figure 4.1 Load-displacement response of specimen (S8-80)

Table 4.1 Specimen (S8-80) details and key load stages

Specimen code: S8-80	GF ratio: 0%	Reinforcement ratio (ρ%): 0.532		
Shear span (a_v): 80 mm	Effective depth (d): 121 mm	$F_{c'}$ (MPa):		f_{st} (MPa): 4.79
		cube	cylinder	
		102.66	92.79	
Load (kN)	Displacement (mm)	Notes		
1	0	Initial seating		
67	0.058	The first hairline cracking		
201	0.966	Peak load failure		
201.9	-	Ultimate bearing capacity		

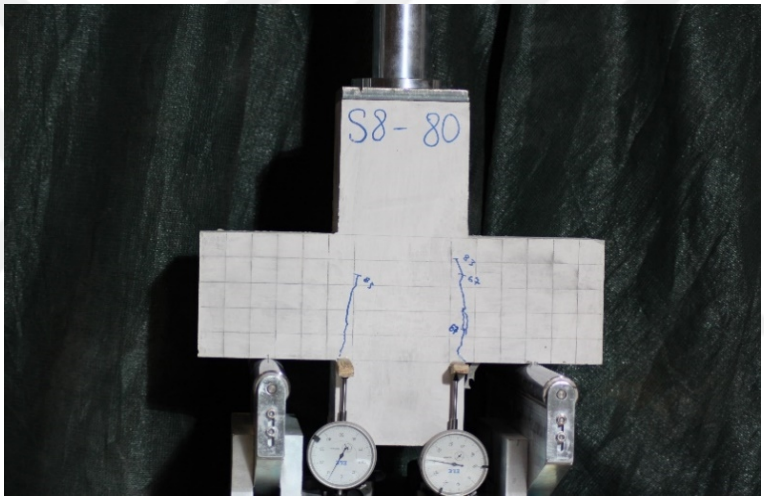

Figure 4.2 Initial cracking of Specimen (S8-80)

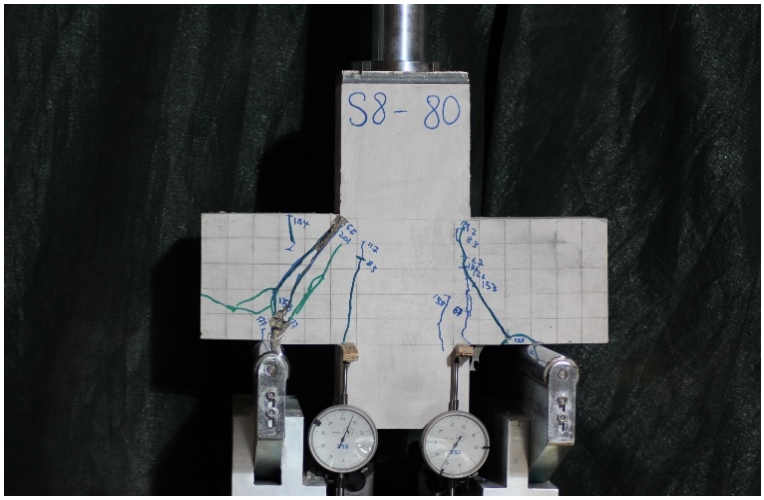

Figure 4.3 Specimen (S8-80) after failure

4.3 Response of Specimen (S8-100)

This specimen has the same properties of the first specimen, the shear span that used in the testing was 100 mm, and the ratio of shear span to the effective depth (a/d) is 0.84. A hairline crack formed on the east side of the corbel at a load of 49 kN followed by another crack on the west side at a load of 66 kN, (see Fig 4.5). Cracks reached the interface between the column and beam of the corbel at a load of 149 kN. Fig. 4.4 shows the load versus displacement response of the tested specimen.

When load reached 112 kN signs of failure appeared and at a load of 143 kN the failure became evident on the east side of the specimen, (see Fig 4.6). The properties of the specimen and the loading key stages are shown in table 4.2. The ultimate bearing capacity was 145.6 kN with total displacement was 1.31 mm. the specimen failed in an explosive manner with a diagonal shear on the east side of the corbel.

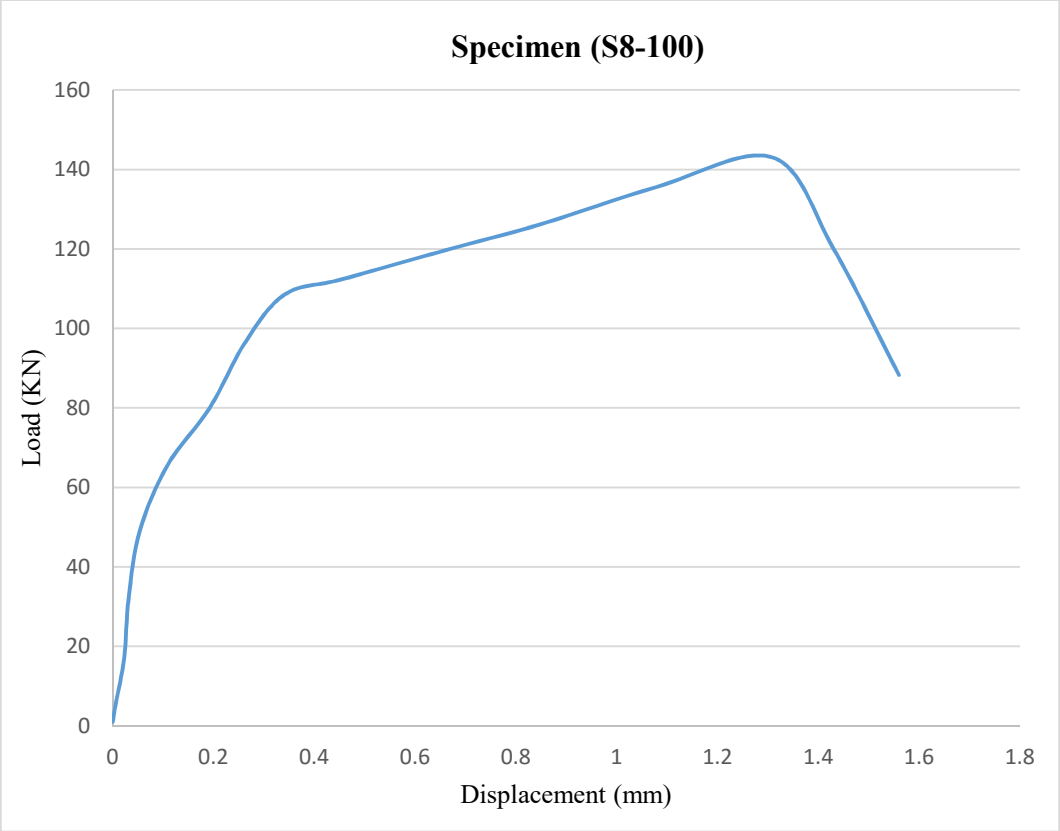

Figure 4.4 Load-displacement response of specimen (S8-100)

Table 4.2 Specimen (S8-100) details and key load stages

<table>
<tr><td>Specimen code:
S8-100</td><td>GF ratio: 0%</td><td colspan="3">Reinforcement ratio (ρ%): 0.563</td></tr>
<tr><td rowspan="2">Shear span (a_v): 100 mm</td><td rowspan="2">Effective depth (d): 119 mm</td><td colspan="2">F_{c}` (MPa):</td><td rowspan="2">f_{st} (MPa): 4.79</td></tr>
<tr><td>cube</td><td>cylinder</td></tr>
<tr><td></td><td></td><td>102.66</td><td>92.79</td><td></td></tr>
<tr><td>Load (kN)</td><td>Displacement (mm)</td><td colspan="3">Notes</td></tr>
<tr><td>1</td><td>0</td><td colspan="3">Initial seating</td></tr>
<tr><td>49</td><td>0.054</td><td colspan="3">The first hairline cracking</td></tr>
<tr><td>143</td><td>1.31</td><td colspan="3">Peak load failure</td></tr>
<tr><td>145.6</td><td>-</td><td colspan="3">Ultimate bearing capacity</td></tr>
</table>

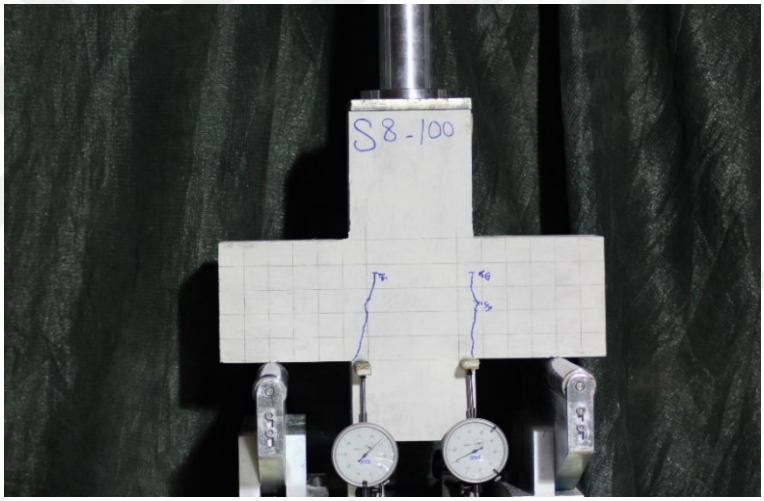

Figure 4.5 Initial cracking of specimen (S8-100)

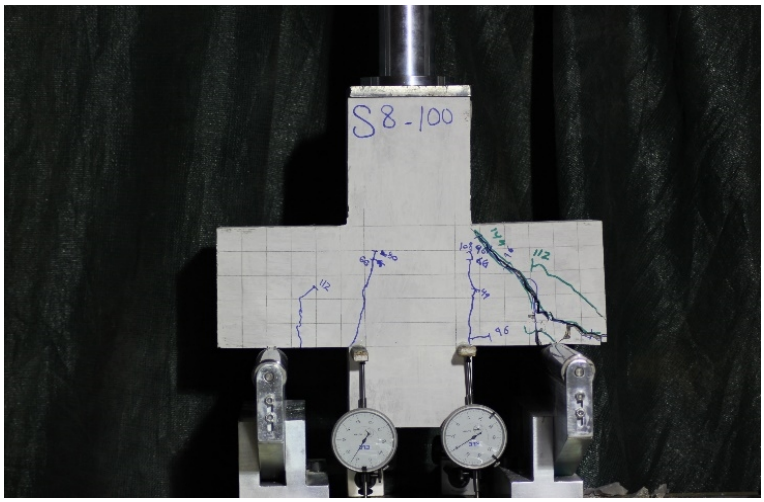

Figure 4.6 Specimen (S8-100) after failure

4.4 Response of Specimen (S8-120)

This specimen made of reinforced concrete and used to study the behavior of high strength concrete and compare it to other specimens reinforced with various glass fiber ratios loaded with vertical load at shear span of 120 mm, it is also used to compare the strengths of concrete corbels without fibers subjected to vertical loads with different shear spans. Fig. 4.7 shows the load – displacement response of the tested specimen.

The First crack was observed at a load of 61 kN on both sides of the corbel, (see Fig. 4.8), those cracks extended to reached the interface between the beam and column of the specimen and followed by diagonal cracks at a load of 98 kN on the west side of the corbel. Failure of the specimen occurred at a load of 123 kN on the west side of the corbel which happened in an explosive manner, (see Fig. 4.9). The total displacement of the corbel equals to 1.142 mm. The Key load stages of the corbel in addition to the details of the specimen are shown in table 4.3.

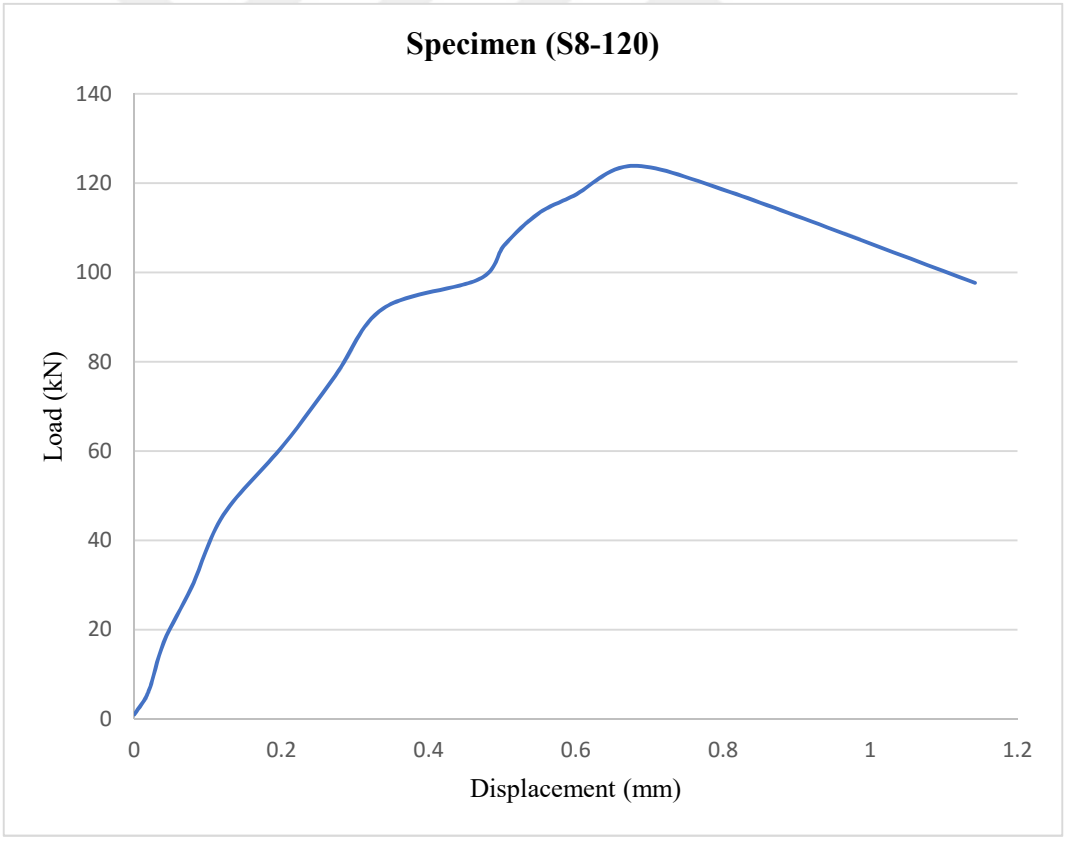

Figure 4.7 Load-displacement response of specimen (S8-120)

Table 4.3 Specimen (S8-120) details and key load stages

<table>
<tr><td>Specimen code: S8-120</td><td>GF ratio: 0%</td><td colspan="3">Reinforcement ratio (ρ%): 0.532</td></tr>
<tr><td rowspan="2">Shear span (a_v): 120 mm</td><td rowspan="2">Effective depth (d): 121 mm</td><td colspan="2">$F_{c'}$ (MPa):</td><td rowspan="2">f_{st} (MPa): 4.79</td></tr>
<tr><td>cube</td><td>cylinder</td></tr>
<tr><td></td><td></td><td>102.66</td><td>92.79</td><td></td></tr>
<tr><td>Load (kN)</td><td>Displacement (mm)</td><td colspan="3">Notes</td></tr>
<tr><td>1</td><td>0</td><td colspan="3">Initial seating</td></tr>
<tr><td>61</td><td>0.203</td><td colspan="3">The first hairline cracking</td></tr>
<tr><td>123</td><td>0.677</td><td colspan="3">Peak load failure</td></tr>
<tr><td>129.8</td><td>-</td><td colspan="3">Ultimate bearing capacity</td></tr>
</table>

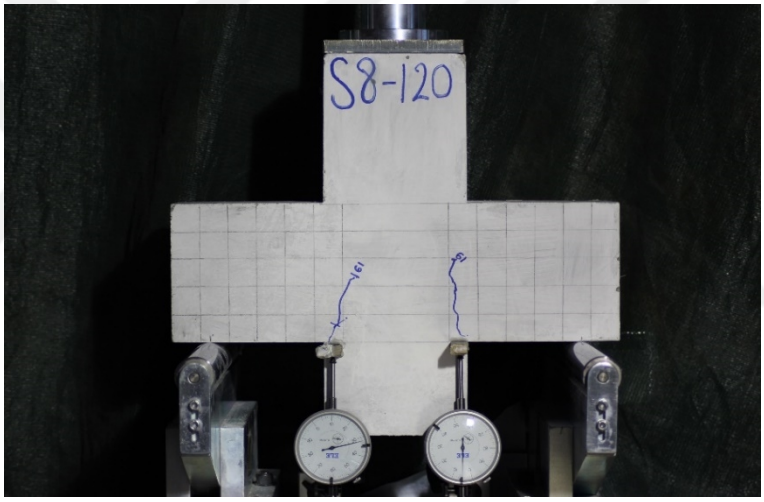

Figure 4.8 Initial cracking of specimen (S8-120)

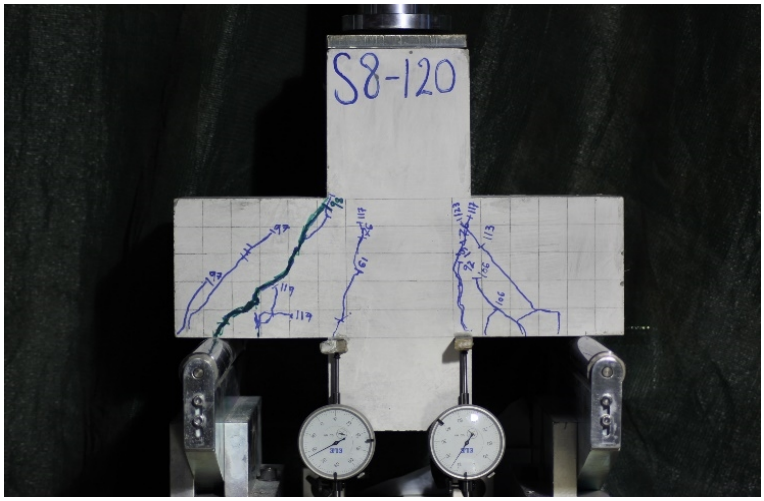

Figure 4.9 Specimen (S8-120) after failure

4.5 Response of Specimen (S8-80-0.2)

Specimen (S8-80-0.2) contained 0.2% by volume of glass fiber. The specimen loaded vertically with a shear span equal to 80 mm. The load–displacement response of the specimen is shown in Fig. 4.10. First hairline crack showed at load of 89 kN on the east side of the corbel another crack formed on the west side at load of 107 kN, (see Fig.4.11), the cracks extended gradually with increasing the load, when load reached 202 kN cracks extended to reach the interface between column and beam on the east side of the corbel.

The Failure occurred at a load of 220 kN on the east side of corbel with displacement in the center equals to 1.385 mm, (see Fig.4.12), the maximum displacement of the corbel was 2.126 mm. the ultimate bearing capacity of the corbel with 0.2% of glass fiber was 221 kN. Table 4.4 shows the details of the specimen with loading keys stages.

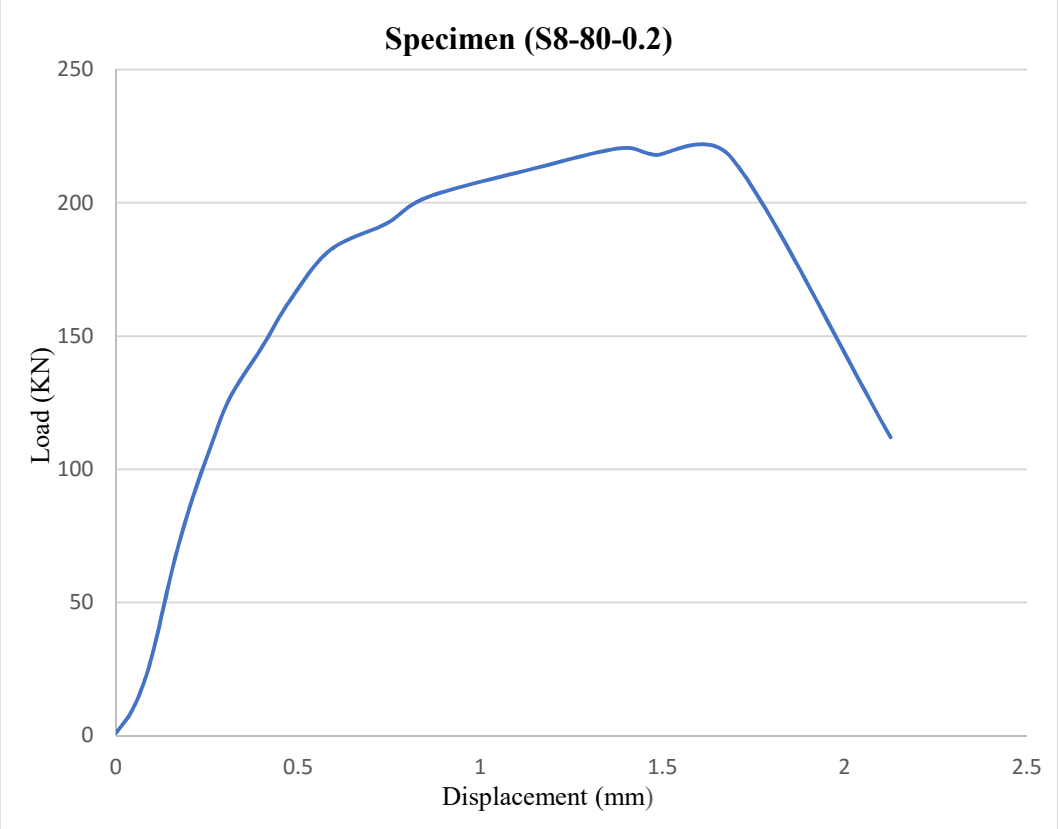

Figure 4.10 Load-displacement response of specimen (S8-80-0.2)

Table 4.4 Specimen (S8-80-0.2) details and key load stages

<table>
<tr><td>Specimen code: S8-80-0.2</td><td>GF ratio: 0.2%</td><td colspan="3">Reinforcement ratio (ρ%): 0.531</td></tr>
<tr><td rowspan="3">Shear span (a_v): 80 mm</td><td rowspan="3">Effective depth (d): 126 mm</td><td colspan="2">$F_{c`}$ (MPa):</td><td rowspan="3">f_{st} (MPa): 4.99</td></tr>
<tr><td>cube</td><td>cylinder</td></tr>
<tr><td>96.15</td><td>83.76</td></tr>
<tr><td>Load (kN)</td><td>Displacement (mm)</td><td colspan="3">Notes</td></tr>
<tr><td>1</td><td>0</td><td colspan="3">Initial seating</td></tr>
<tr><td>89</td><td>0.211</td><td colspan="3">The first hairline cracking</td></tr>
<tr><td>220</td><td>1.385</td><td colspan="3">Peak load failure</td></tr>
<tr><td>221</td><td>-</td><td colspan="3">Ultimate bearing capacity</td></tr>
</table>

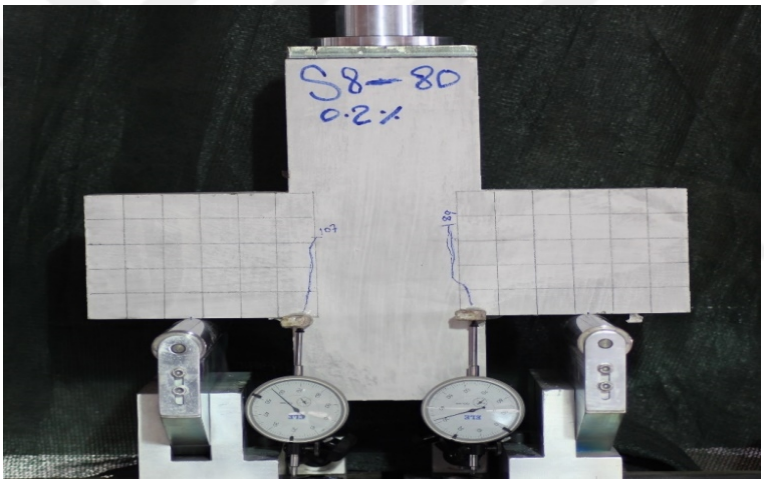

Figure 4.12 Initial cracking of specimen (S8-80-0.2)

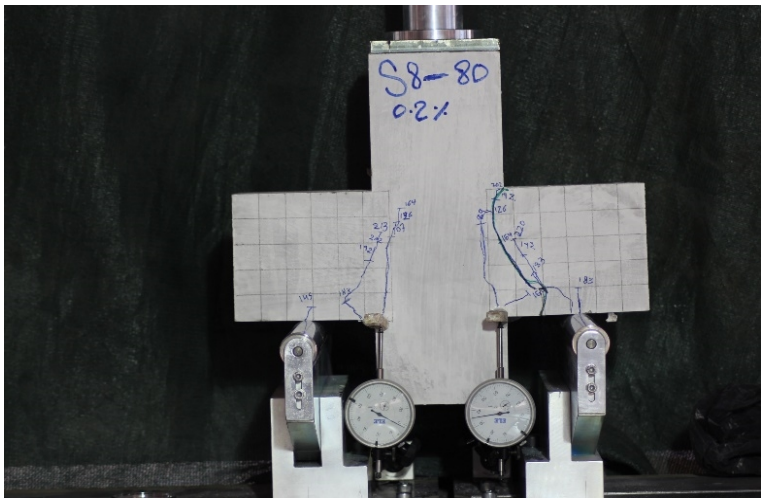

Figure 4.11 Specimen (S8-80-0.2) after failure

4.6 Response of Specimen (S8-100-0.2)

This specimen had identical properties to the previous specimen which it reinforced with 0.2 % by volume of glass fiber, the corbel was loaded with vertical load with a shear span of 100 mm. Fig. 4.13 showing the displacement-load response of the corbel. The first hairline crack appeared at a load of 67 kN on the west side of the specimen another crack appeared at a load of 86 kN on the other side of the specimen, (see Fig 4.14), cracks reached the interface between the column and beam 149 kN on the west side of the specimen.

When the load reached 175 failure occurred on the west side of the specimen with displacement equal to 1.70 mm, (see Fig 4.15), the maximum displacement of the sample in the center of the corbel was 1.97 mm. the properties of the specimen with load key stages are shown in table 4.5.

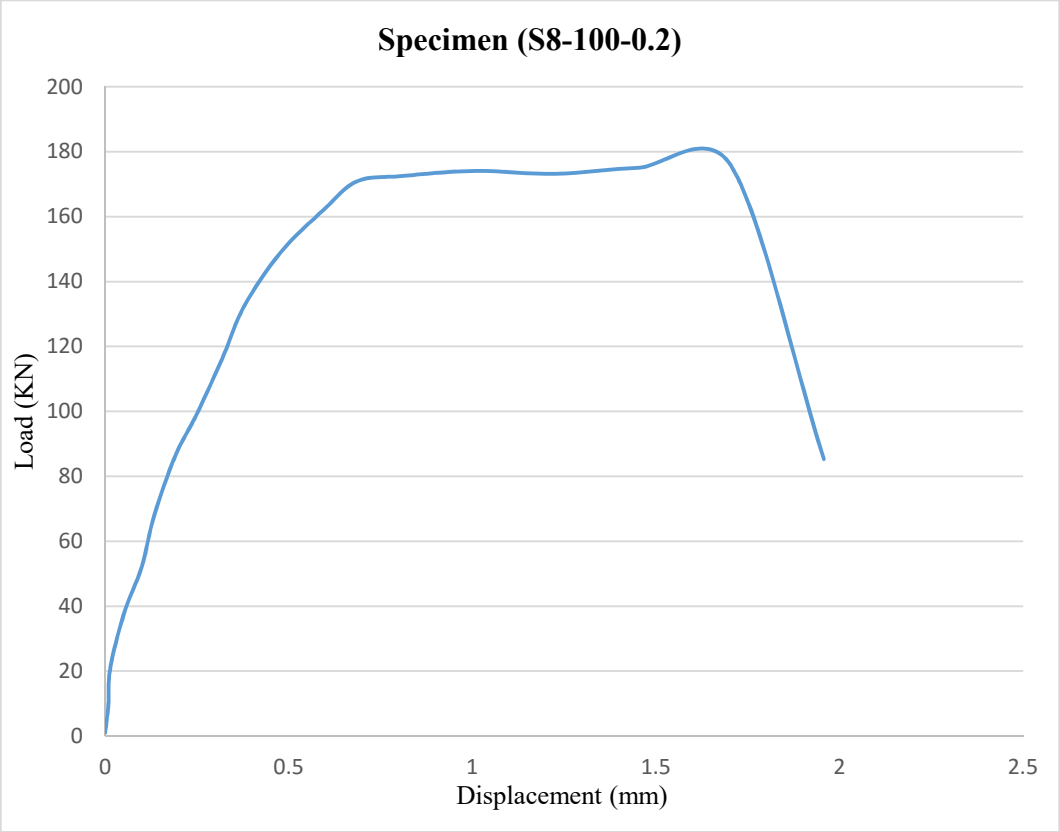

Figure 4.13 Load-displacement response of specimen (S8-100-0.2)

Table 4.5 Specimen (S8-100-0.2) details and key load stages

<table>
<tr><td>Specimen code: S8-100-0.2</td><td>GF ratio: 0.2%</td><td colspan="3">Reinforcement ratio (ρ%): 0.536</td></tr>
<tr><td rowspan="2">Shear span (a_v): 100 mm</td><td rowspan="2">Effective depth (d): 125 mm</td><td colspan="2">$F_{c'}$ (MPa):</td><td rowspan="2">f_{st} (MPa): 4.99</td></tr>
<tr><td>cube</td><td>cylinder</td></tr>
<tr><td></td><td></td><td>96.15</td><td>83.76</td><td></td></tr>
<tr><td>Load (kN)</td><td>Displacement (mm)</td><td colspan="3">Notes</td></tr>
<tr><td>1</td><td>0</td><td colspan="3">Initial seating</td></tr>
<tr><td>67</td><td>0.134</td><td colspan="3">The first hairline cracking</td></tr>
<tr><td>175</td><td>1.70</td><td colspan="3">Peak load failure</td></tr>
<tr><td>176</td><td>-</td><td colspan="3">Ultimate bearing capacity</td></tr>
</table>

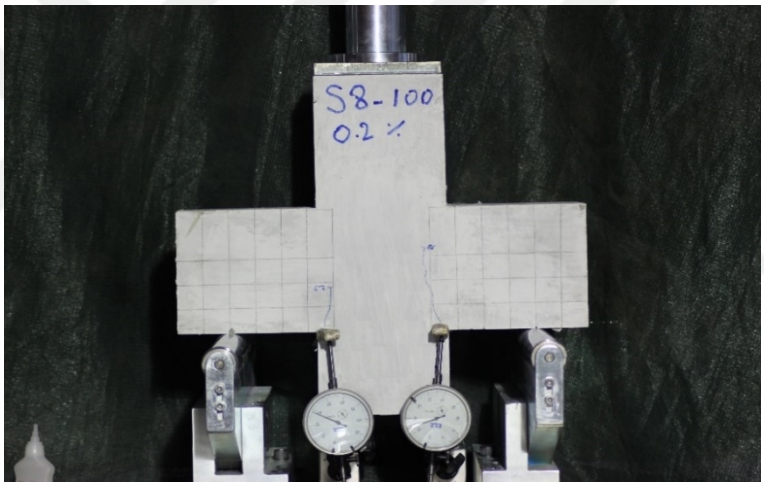

Figure 4.14 Initial cracking of specimen (S8-100-0.2)

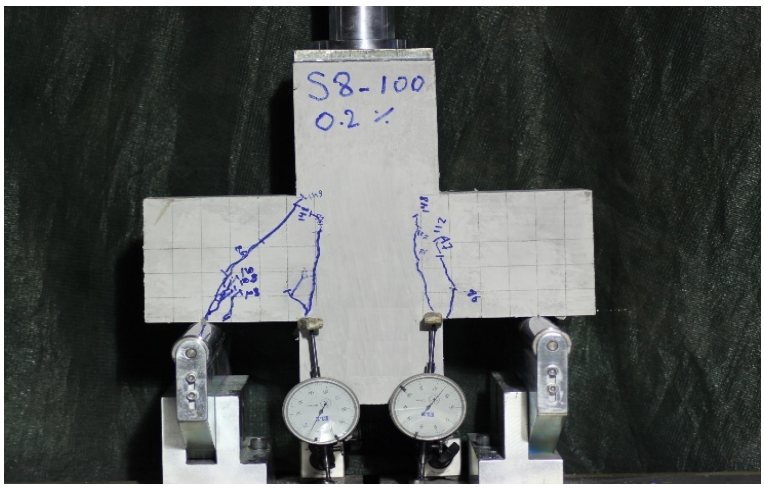

Figure 4.15 Specimen (S8-100-0.2) after failure

4.7 Response of Specimen (S8-120-0.2)

This specimen was subjected to vertical load with a shear span equal to 120 mm, shear span to the effective depth ratio (a/d) equals 0.95. The load-displacement of the specimen is shown in Fig. 4.16. Hairline cracks appeared on both side of the specimen at a load of 59 kN, (see Fig. 4.17), These cracks reached the center of the beam of the corbel at a load of 71 kN. When load reached 112 kN a crack extended to reach the interface between column and beam on the west side of the specimen, another crack was formed on the east side of the specimen at a load of 138 kN.

Specimen failed at a load of 143 kN with shear crack formed on the east side of the corbel with a displacement of 2.4 mm in the center, (see Fig. 4.18), the maximum displacement of the corbel reached to 2.538 mm. table 4.6 shows the key load stages and details of the specimen.

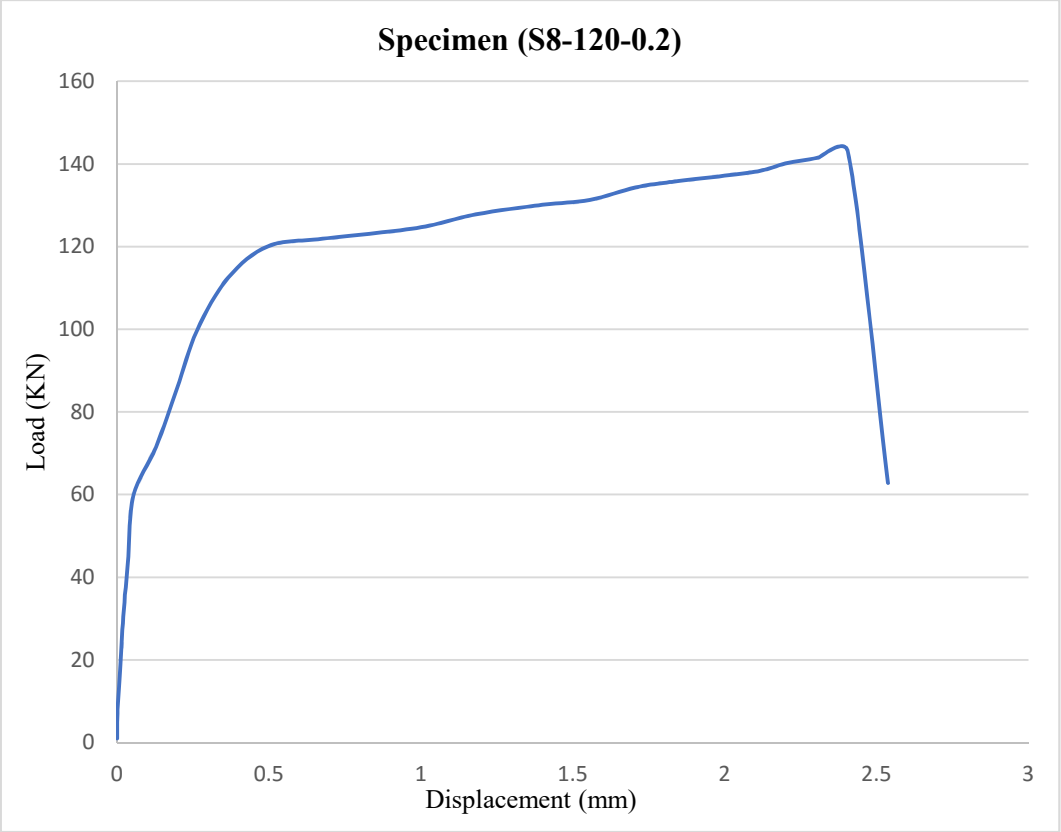

Figure 4.16 Load-displacement response of specimen (S8-120-0.2)

Table 4.6 Specimen (S8-120-0.2) details and key load stages

<table>
<tr><td>Specimen code: S8-120-0.2</td><td>GF ratio: 0.2%</td><td colspan="3">Reinforcement ratio (ρ%): 0.531</td></tr>
<tr><td rowspan="2">Shear span (a_v): 120 mm</td><td rowspan="2">Effective depth (d): 126 mm</td><td colspan="2">$F_{c'}$ (MPa):</td><td rowspan="2">f_{st} (MPa): 4.99</td></tr>
<tr><td>cube</td><td>cylinder</td></tr>
<tr><td></td><td></td><td>96.15</td><td>83.76</td><td></td></tr>
<tr><td>Load (kN)</td><td>Displacement (mm)</td><td colspan="3">Notes</td></tr>
<tr><td>1</td><td>0</td><td colspan="3">Initial seating</td></tr>
<tr><td>59</td><td>0.053</td><td colspan="3">The first hairline cracking</td></tr>
<tr><td>143</td><td>2.40</td><td colspan="3">Peak load failure</td></tr>
<tr><td>143.6</td><td>-</td><td colspan="3">Ultimate bearing capacity</td></tr>
</table>

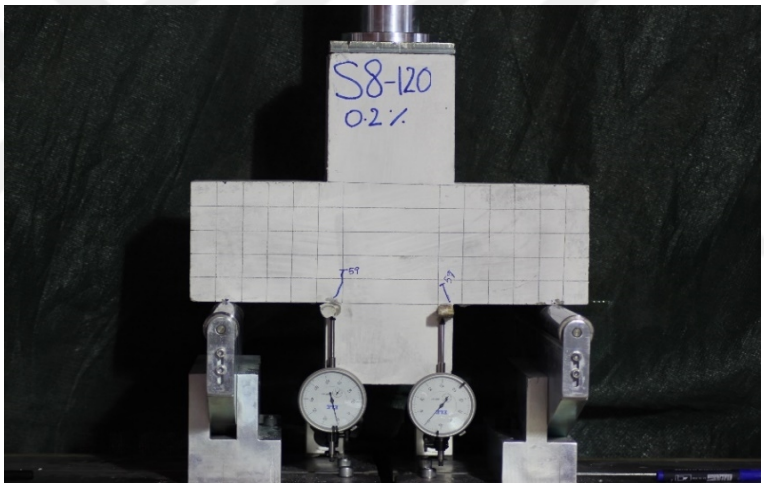

Figure 4.18 Initial cracking of specimen (S8-120-0.2)

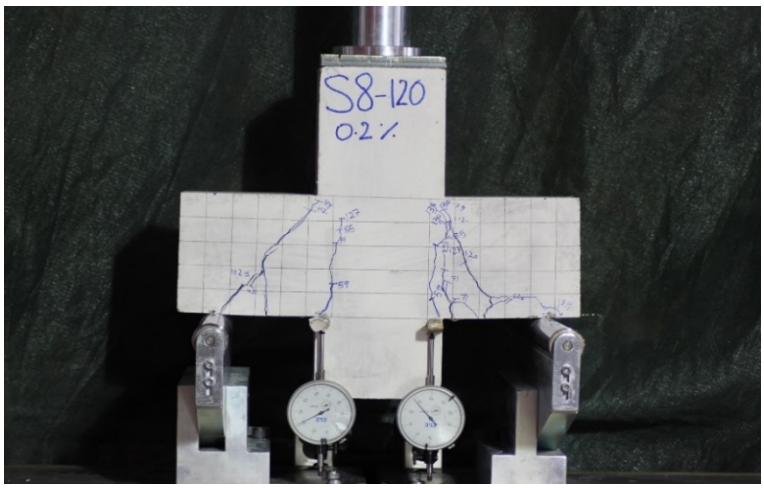

Figure 4.17 Specimen (S8-120-0.2) after failure

4.8 Response of Specimen (S8-80-0.4)

Specimen (S8-80-0.4) was reinforced with 0.4% by volume with glass fiber, this specimen used as comparison specimen to other specimens reinforced with various glass fiber ratios loaded with vertical load at shear span of 80 mm, it is also used to compare the strengths of concrete corbels reinforced with 0.4% by volume of glass fibers subjected to vertical loads with different shear spans. Fig. 4.19 shows the load–displacement response of the tested specimen.

First hairline crack appeared in the specimen at load of 78 kN on the east side of the corbel, on the other side of the specimen crack showed at load of 113 kN, (see Fig. 4.20), cracks extended to reach the interface between the column and beam on the east side of specimen at load 225 kN, (see Fig. 4.21), the ultimate bearing capacity of the specimen was 228 kN. The maximum displacement in the center of the specimen equals to 2.28 mm. Table 4.7 shows the details of the specimen with loading keys stages.

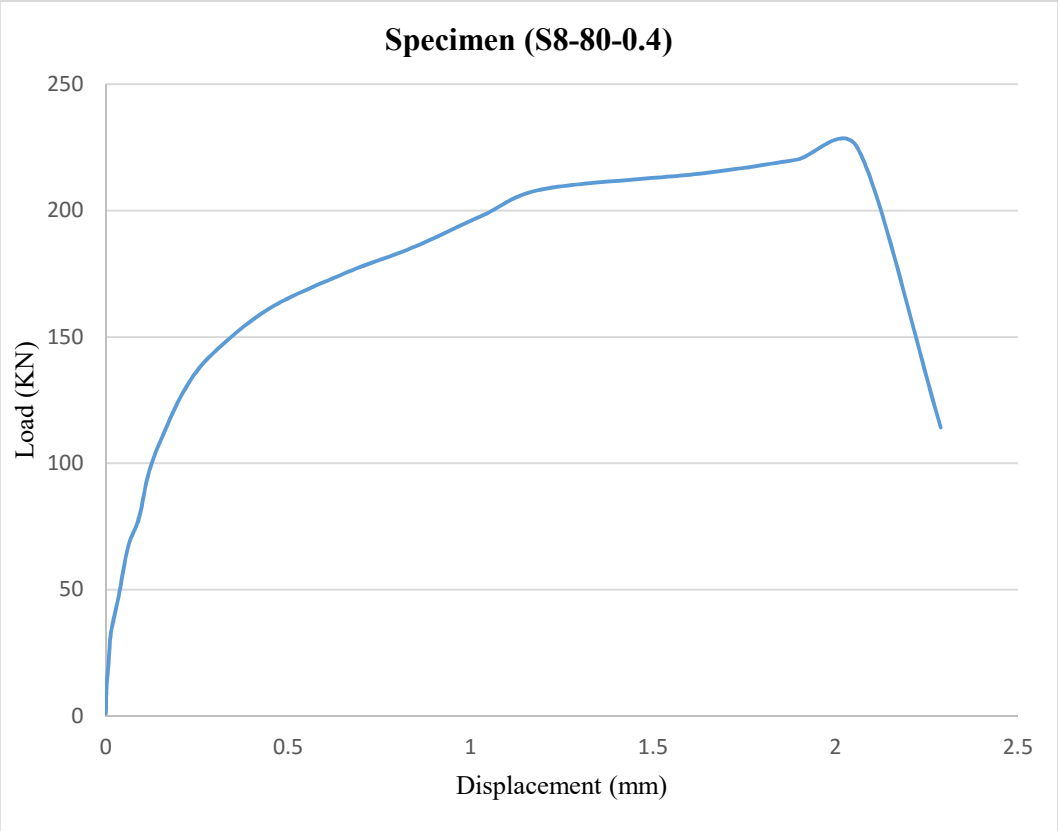

Figure 4.19 Load-displacement response of specimen (S8-80-0.4)

Table 4.7 Specimen (S8-80-0.4) details and key load stages

Specimen code: S8-80-0.4	GF ratio: 0.4%	Reinforcement ratio (ρ%): 0.531		
Shear span (a_v): 80 mm	Effective depth (d): 126 mm	$F_{c'}$ (MPa):		f_{st} (MPa): 5.14
		cube	cylinder	
		98.69	88.26	
Load (kN)	Displacement (mm)	Notes		
1	0	Initial seating		
78	0.091	The first hairline cracking		
224	2.06	Peak load failure		
228	-	Ultimate bearing capacity		

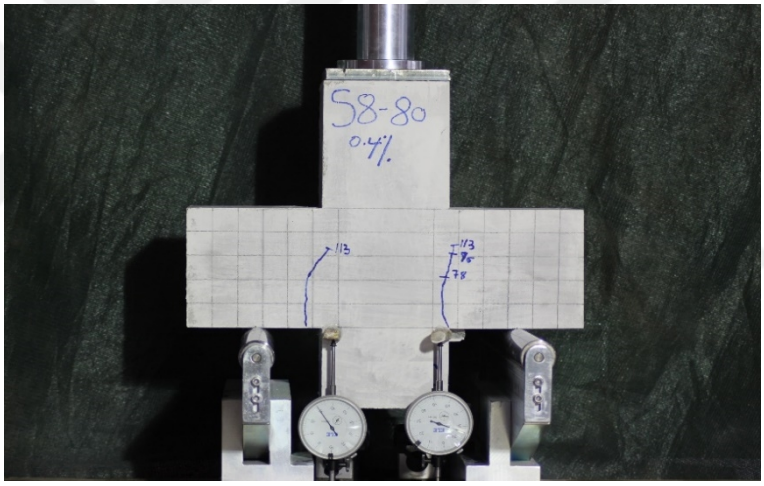

Figure 4.21 Initial cracking of specimen (S8-80-0.4)

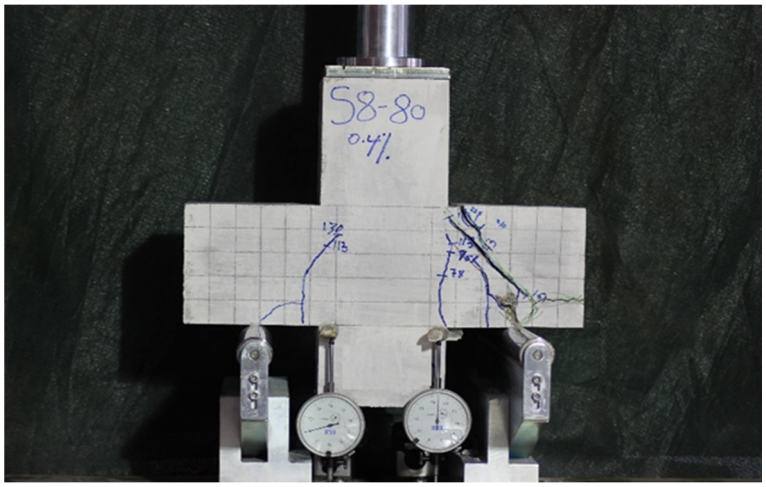

Figure 4.20 Specimen (S8-80-0.4) after failure

4.9 Response of Specimen (S8-100-0.4)

This specimen was reinforced with the same amount of glass fiber as the previous specimen which is 0.4% by volume. A shear span of 100 mm was used during the test, the corbel was loaded vertically. At a load of 63 kN and 80 kN, cracks appeared on the east and west side of the specimen, respectively. These cracks extended to cross the center of the corbel at load equals to 96 kN. Fig. 4.22 shows the load-displacement response of the specimen.

The specimen failed at a load of 195 kN with maximum displacement in the middle of the corbel equals 3.31 mm, Figs. (4.23, 4.24) showing the initial cracking and failure of the specimen. The ultimate bearing capacity of this specimen was 197 kN. Table 4.8 shows the key load stages with the characteristics of the specimen.

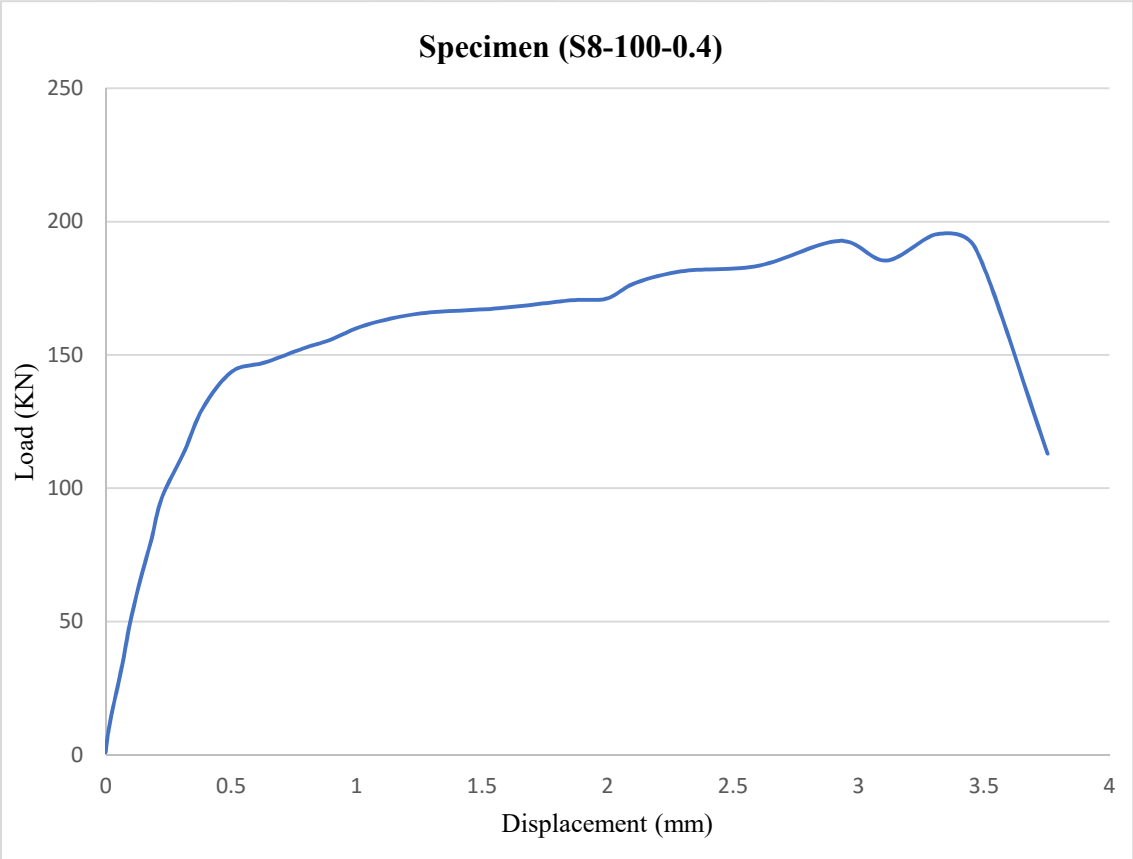

Figure 4.22 Load-displacement response of specimen (S8-100-0.4)

Table 4.8 Specimen (S8-100-0.4) details and key load stages

Specimen code: S8-100-0.4	GF ratio: 0.4%	Reinforcement ratio (ρ%): 0.536	
Shear span (a_v): 100 mm	Effective depth (d): 125 mm	$F_{c'}$ (MPa): cube: 98.69; cylinder: 88.26	f_{st} (MPa): 5.14
Load (kN)	Displacement (mm)	Notes	
1	0	Initial seating	
63	0.133	The first hairline cracking	
195	3.314	Peak load failure	
197	-	Ultimate bearing capacity	

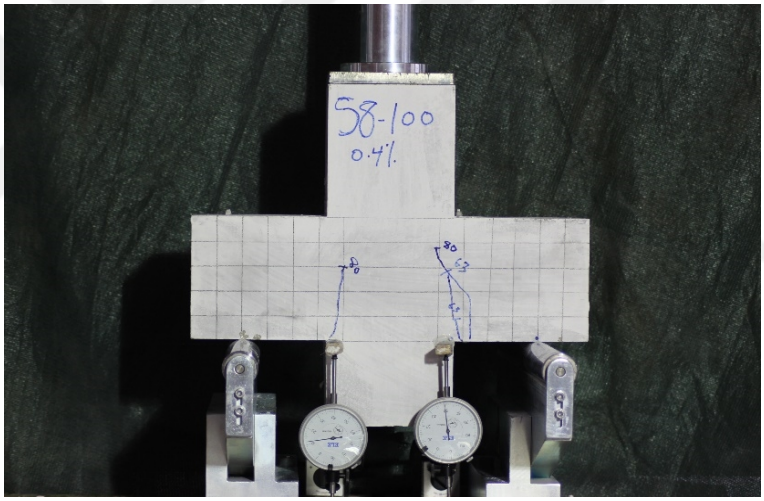

Figure 4.24 Initial cracking of specimen (S8-100-0.4)

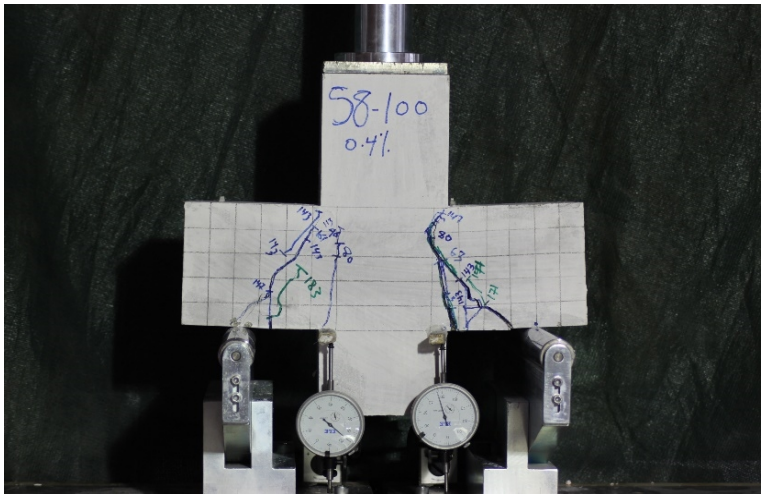

Figure 4.23 Specimen (S8-100-0.4) after failure

4.10 Response of Specimen (S8-120-0.4)

Specimen (S8-120-0.4) contained 0.4% by volume of glass fiber. The corbel tested by the vertical load, 120 mm shear span was used, shear span to the effective depth ratio (a_v/d) was 0.95. Fig. 4.25 shows the load-displacement response of the specimen. On the east side of the corbel beam, a hairline crack appeared at load equals to 59 kN. On the other side of the beam a crack occurred at a load of 75 kN, these cracks spread and crossed the center of the beam at a load of 85 kN.

The specimen failed at a load of 147 kN on the east side of the corbel with displacement in the center equals to 1.71 mm, the ultimate bearing capacity of the corbel was 154 kN, and the maximum displacement of the specimen was 2.73 mm. table 4.9 shows the properties of the specimen with key load stages. Figs. (4.26, 4.27) showing the initial cracking and failure of the specimen.

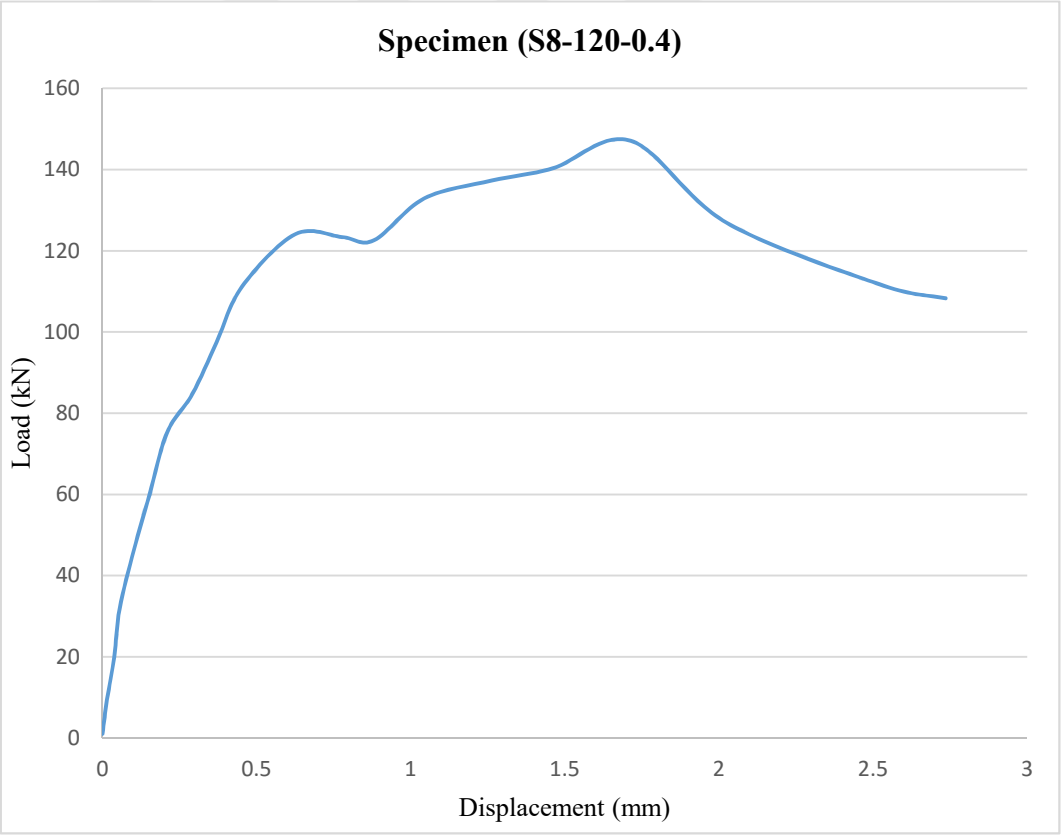

Figure 4.25 Load-displacement response of specimen (S8-120-0.4)

Table 4.9 Specimen (S8-120-0.4) details and key load stages

<table>
<tr><td>Specimen code: S8-120-0.4</td><td>GF ratio: 0.4%</td><td colspan="3">Reinforcement ratio (ρ%): 0.536</td></tr>
<tr><td rowspan="2">Shear span (a_v): 120 mm</td><td rowspan="2">Effective depth (d): 125 mm</td><td colspan="2">$F_{c'}$ (MPa):</td><td rowspan="2">f_{st} (MPa): 5.14</td></tr>
<tr><td>cube</td><td>cylinder</td></tr>
<tr><td></td><td></td><td>98.69</td><td>88.26</td><td></td></tr>
<tr><td>Load (kN)</td><td>Displacement (mm)</td><td colspan="3">Notes</td></tr>
<tr><td>1</td><td>0</td><td colspan="3">Initial seating</td></tr>
<tr><td>59</td><td>0.15</td><td colspan="3">The first hairline cracking</td></tr>
<tr><td>147.1</td><td>1.71</td><td colspan="3">Peak load failure</td></tr>
<tr><td>152.6</td><td>-</td><td colspan="3">Ultimate bearing capacity</td></tr>
</table>

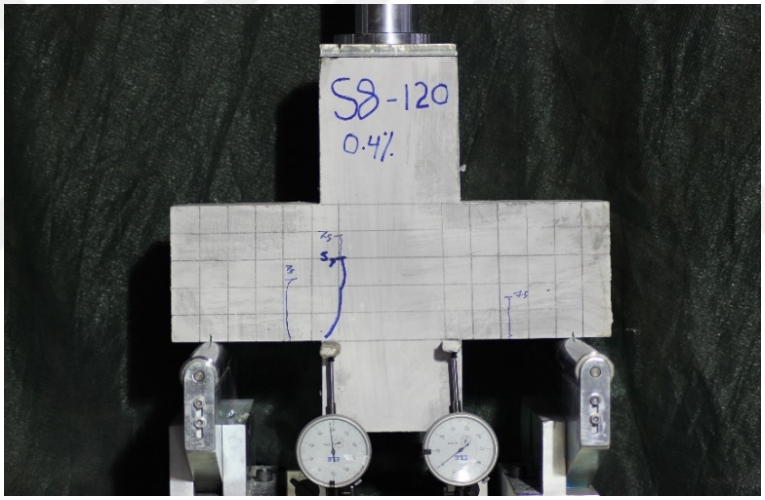

Figure 4.27 Initial cracking of specimen (S8-120-0.4)

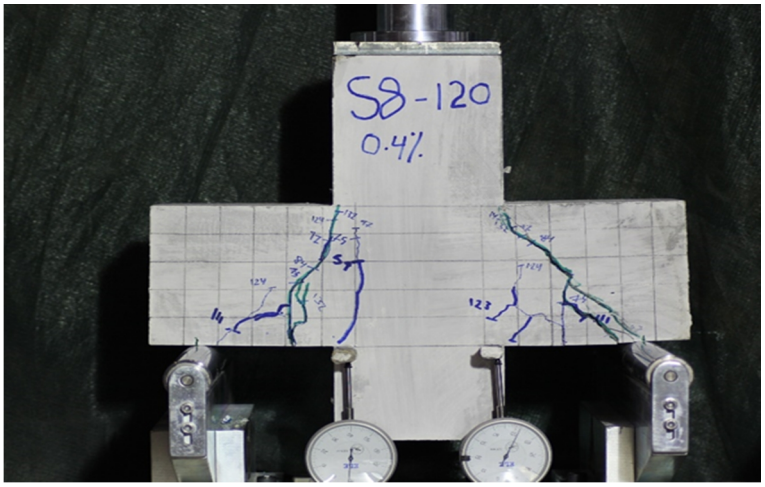

Figure 4.26 Specimen (S8-120-0.4) after failure

4.11 Results Comparison

4.11.1 Effect of glass fiber percentage

In many specimens that reinforced with glass fiber, a remarkable enhancement in the ductility was noted compared to the specimens without glass fiber. This improvement in the ductility due to the glass fiber was observed with different shear spans. When fibers are present, a significant post-cracking strength that led to maximum deflection which can be observed in figs clearly.

In the absence of fibers, crushing of concrete (sudden failure) occurs before the yielding of main steel and brittle behavior is evident, in most of the tested specimens there is no available ductility (see Figs 4.28, 4.29 and 4.30) . When fibers are added available ductility increased and the increments becomes more evident by increasing the percentage of glass fiber. The shear strength of corbels was greatly increased with the addition of fibers. However, the mode of failure was sudden even after the addition of glass fibers.

Another important advantage of the addition of glass fiber is the improvement in the load bearing capacity of corbels can be noted clearly. The increment in the capacity is pronounced more as compared to the sample without glass to the same sample with glass fiber. Therefore, a general conclusion can be made that the load bearing capacity of the specimen by increasing the fiber percentage in the concrete.

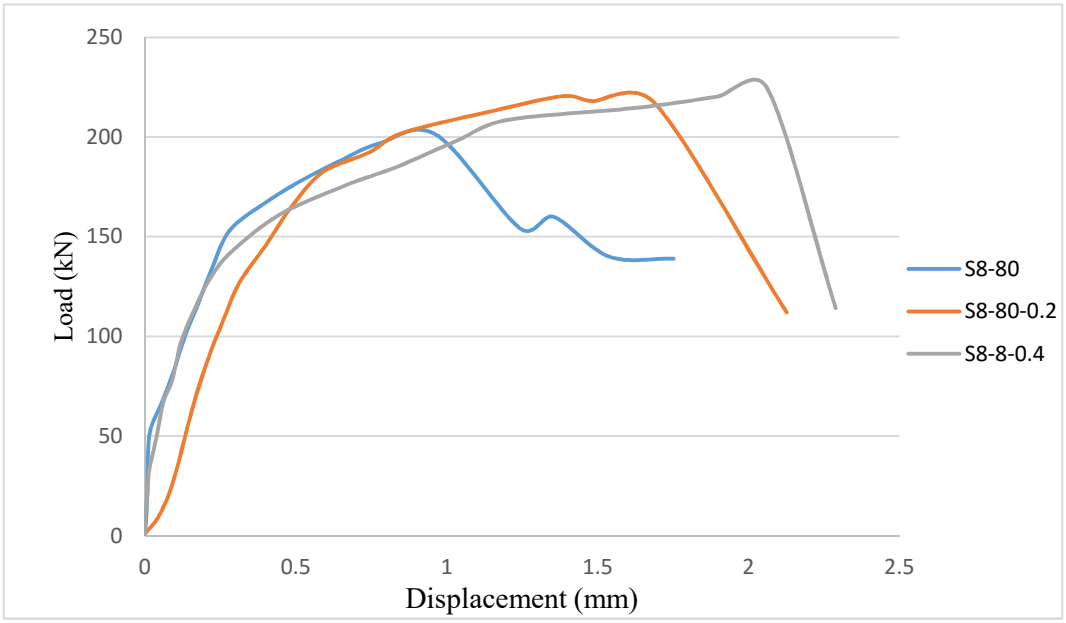

Figure 4.28 Load bearing capacity of corbels with different glass fiber ratios (a=80 mm)

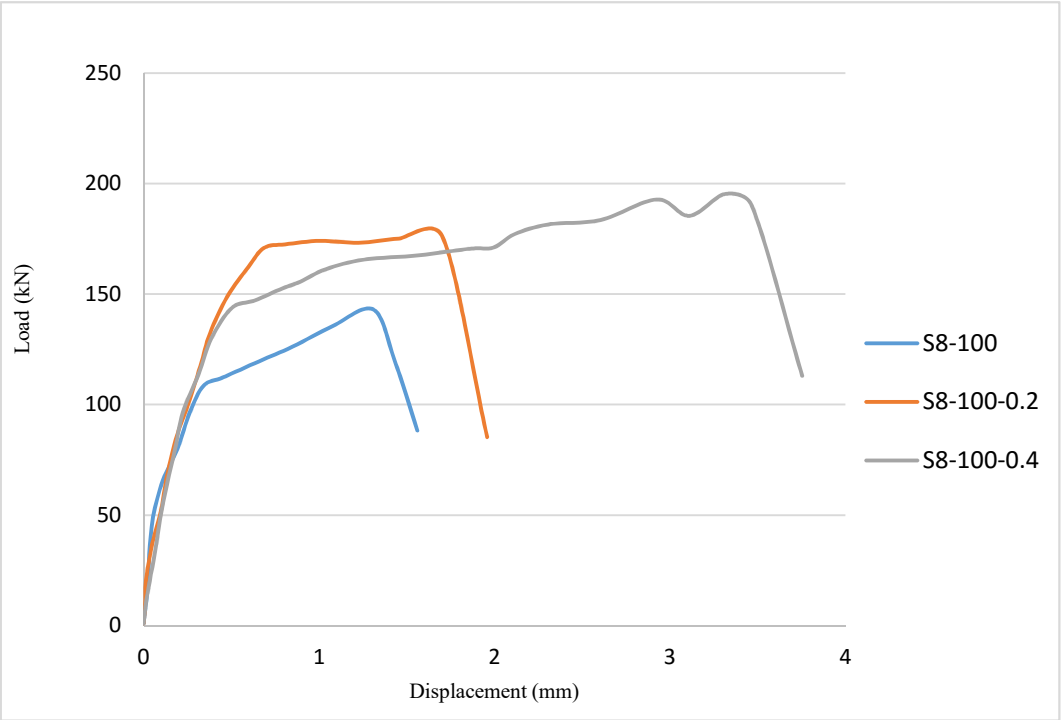

Figure 4.30 Load bearing capacity of corbels with different glass fiber ratios (a=100 mm)

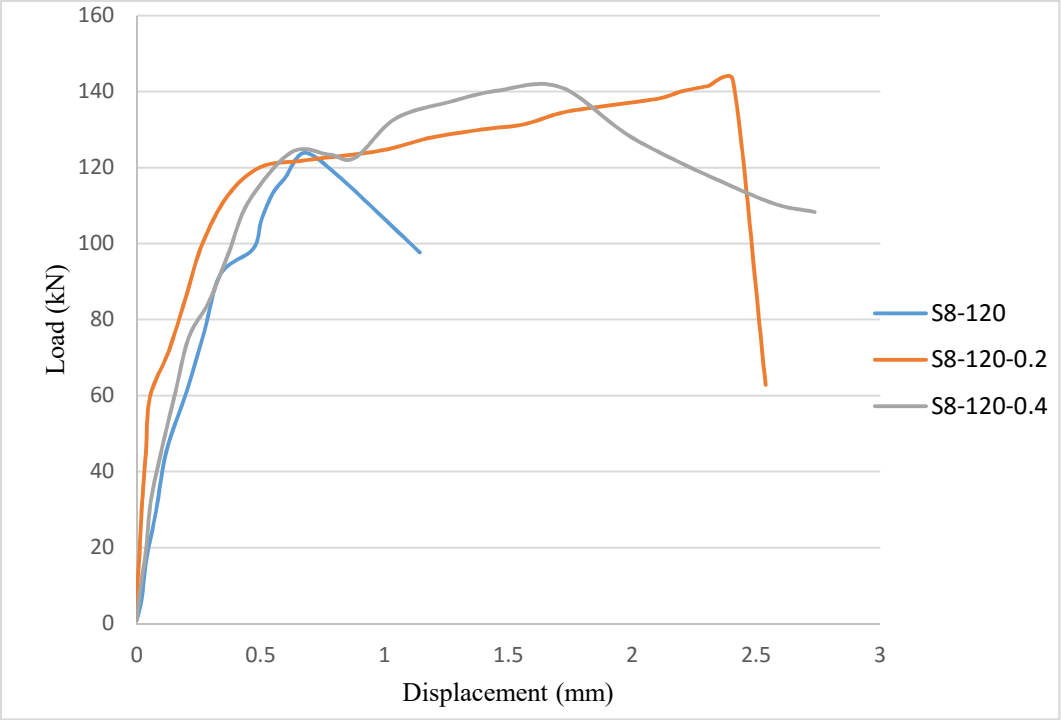

Figure 4.29 Load bearing capacity of corbels with different glass fiber ratios (a=120 mm)

4.11.2 Effect of shear span

Shear span is an important parameter which has a significant effect on the bearing capacity of the corbels. Generally, the carrying capacity of corbel decreases by increasing the shear span. However, the influence of the shear span is related to the effective depth. Therefore, the effect of shear span to the effective depth ratio (a/d) on the corbels is adopted by many studies.

According to the results there is a significant reduction in the strength of the specimens with glass fiber and without glass fiber as the shear span increased. Figs. (4.31, 4.32 and 4.33) shows the effect of the shear span on the tested specimen.

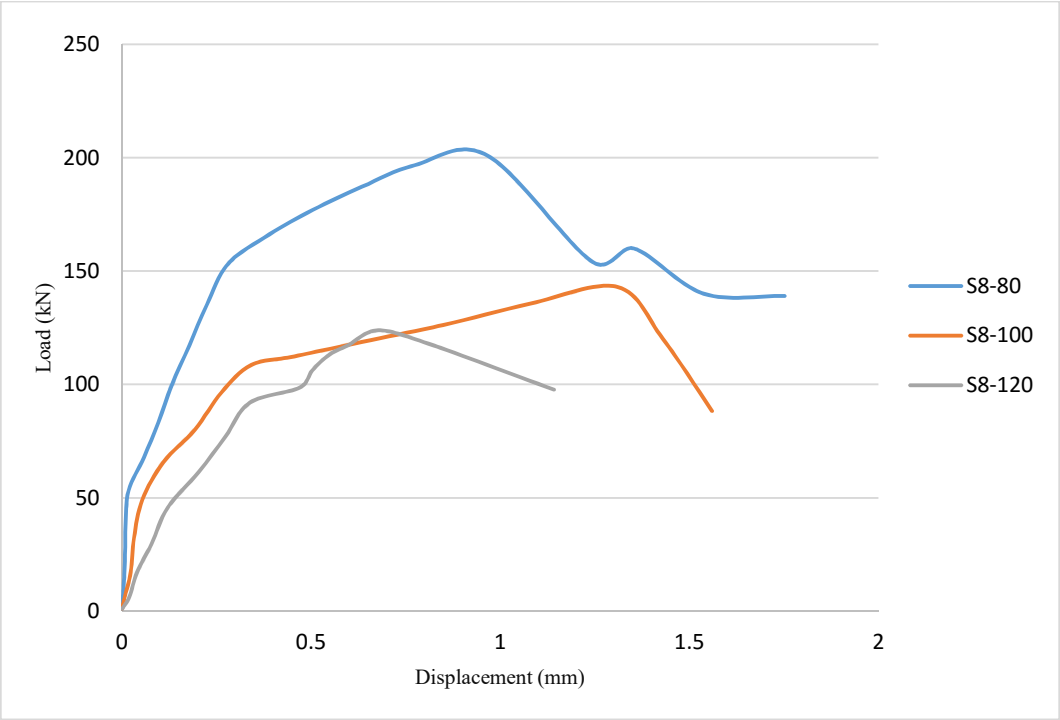

Figure 4.31 Effect of shear span on the load bearing capacity of corbels (vf =0%)

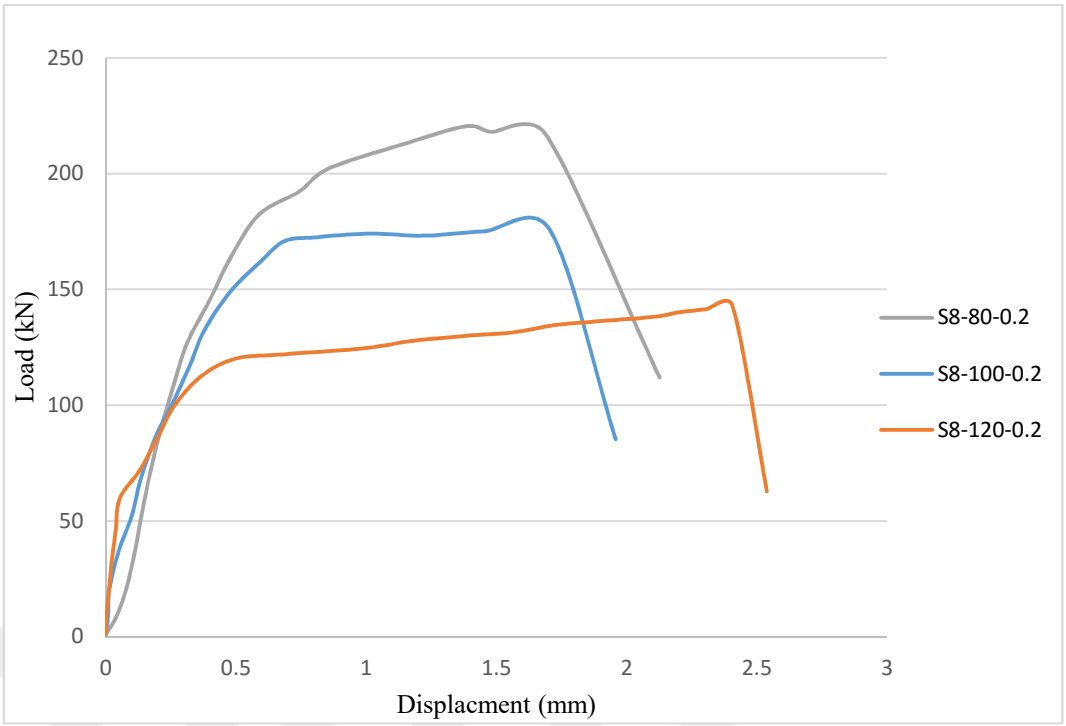

Figure 4.32 Effect of shear span on the load bearing capacity of corbels (vf =0.2%)

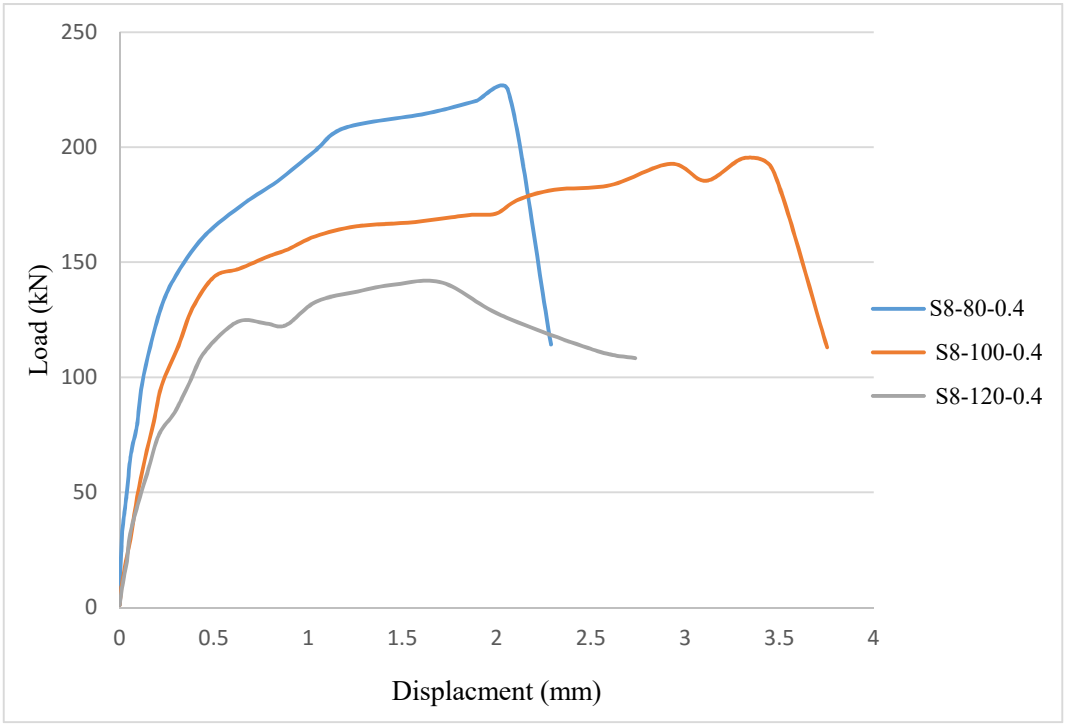

Figure 4.33 Effect of shear span on the load bearing capacity of corbels (vf =0.4%)

CHAPTER 5

CONCLUSION

5.1 Conclusion

Corbels are widely used in precast construction, due to the important of this element many studies have been conducted on the behavior of the corbel. However, there are no studies have been made to explain the effect of glass fiber addition to high strength concrete corbels. This is the first experimental investigation that presents and evaluate the response of high strength corbel reinforced with glass fiber loaded with vertical loads. The following subjects are presented in this thesis:

- A detailed literature review on corbels design and fibrous corbels.
- An experimental investigation on high strength concrete corbels reinforced with glass fiber.
- Analysis of results and discussion of specimens' response.

Corbels can be considered as short cantilever which acts like simple trusses or deep beams which it designed for shear. Corbels are used to support precast beams at the column, therefore, the ductility and the strength of the corbel are more crucial compared with other structural members. Based on the results of the experimental investigation following conclusions can be drawn.

1. The addition of small percentage glass fibers (0.2-0.4) to high strength concrete corbels enhanced the bearing capacity of corbels significantly compared to the corbels without fibers.
2. The mode of failure of corbels was sudden even after the addition of the glass fiber.

3. Another important advantage of addition of glass fiber Shear-transfer corbels with glass fibers have shown a significant post cracking strength, and also have shown more ductility.

4. Results showed that increasing of the shear span can decrease the load carrying capacity remarkably.

5. The cracking of glass fiber reinforced specimens were slower compared to the plain specimens, moreover, the fibrous corbels has much smaller crack width as compared to corbels without glass fiber this reduction leads to long service life which a desirable characteristic in corbels design.

5.2 Recommendations for Future Research

Understanding the structural behavior of high strength concrete corbels with and without glass fiber reinforcement needs fundamental studies to be performed on similar specimens with different parameters other than reported here. In this thesis, the effect of some variables such as glass fiber ratio, varied shear spans were studied under a vertical load. Other variables not reported in this study and under a combination of both horizontal and vertical loading deserve special attention.

A combination of vertical and horizontal loading should be used to investigate the variations of shear span and other variables such as glass fiber ratios and steel ratios.

Tests were done at span (80,100 and 120) mm. More investigation is needed to determine the effects of shear span outside these values.

The results were based upon a limited number of specimens, therefore, precise conclusions may not be easily drawn. More work is still needed on high strength concrete specimens with and without glass fibers and cube strength ranging between 70 MPa to 100 MPa, before reaching a general conclusion.

Furthermore, since in this study only a limited test specimen was carried out with different compressive strength with and without glass fibers, therefore the effect of concrete strength on stress-strain relationship which was left to other researchers to investigate.

Also, further tests on shear-transfer strength specimens are also needed. Further tests on cracked specimens with different strengths and glass ratios are also important to study the rehabilitation of these specimen.

Since corbels are significant structural elements in industrial buildings and industrial buildings are likely to exposure to fire. Fire performance of reinforced concrete and glass fiber reinforced concrete can be researched and necessary measures can be taken into account before a possible fire by strengthening and rehabilitation processes.

REFERENCES

Abdul-Razzak, A. A., Ali, A. A. M. (2011). Influence of cracked concrete models on the nonlinear analysis of high strength steel fibre reinforced concrete corbels, *Composite Structures*, **93**(9), 2277–2287.

Abdul-Razzak, A. A., Mohammed Ali, A. A. (2011). Modelling and numerical simulation of high strength fibre reinforced concrete corbels, *Applied Mathematical Modelling*, **35**(6), 2901–2915.

ACI 318 (2015). Building code requirements for structural concrete and commentary, American Concrete Institute; Farmington Hills, MI, USA.

Ashraf H. Elzanaty, Arthur H. Nilson, and F. O. S. (1986). Shear capacity of reinforced concrete beams using high-strength concrete, *ACI Journal Proceedings*, **83**(2), 290–296.

Campione, G. (2005). Flexural behaviour of concrete corbels containing steel fibers or wrapped with FRP sheets, *Materials and Structures*, **38**(280), 617–625.

Campione, G. (2009). Flexural response of FRC corbels, *Cement and Concrete Composites*, **31**(3), 204–210.

Campione, G., La Mendola, L., Mangiavillano, M. L. (2007). Steel fiber-reinforced concrete corbels: Experimental behavior and shear strength prediction, *ACI Structural Journal*, **104**(5), 570–579.

Chandramouli K., Rao, S. S., Pannirselvam N, Sekhar, S. T., Sravana P. (2010). Strength properties of glass fibre concrete, *Journal of Engineering and Applied Sciences*, **5**(4), 1–6.

Choi, Y., Yuan, R. L. (2005). Experimental relationship between splitting tensile strength and compressive strength of GFRC and PFRC, *Cement and Concrete Research*, **35**, 1587–1591.

Fattuhi, N. I. (1990). Column-load effect on reinforced concrete corbels, *ACI Structural Journal*, **116**(1), 188–197.

Fattuhi, N. I. (1994). Reinforced corbels made with plain and fibrous concretes. *ACI Structural Journal*, *91*(5), 530–536.

Najim, KB. (2002). Using high performance steel fibre concrete to improve the impact strength property, M. Sc, Thesis, Military College of Engineering, Baghdad.

Khalifa, E. S. (2012). Macro-mechanical strut and tie model for analysis of fibrous high-strength concrete corbels, *Ain Shams Engineering Journal*, **3**(4), 359–365.

Kizilkanat, A. B., Kabay, N., Akyüncü, V., Chowdhury, S., Akça, A. H. (2015). Mechanical properties and fracture behavior of basalt and glass fiber reinforced concrete : An experimental study, *Construction and Building Materials*, **100**, 218–224.

Kriz, L. B., Raths, C. H. (1965). Connections in precast concrete Structures—Strength of corbels, *PCI Journal*, **10**(1), 16–61.

Kumar, S., Barai, S. V. (2010). Neural networks modeling of shear strength of SFRC corbels without stirrups, *Applied Soft Computing Journal*. **10**(1):135-148.

Kumar, S. (2005). Shear strength of reinforced steel fibrous concrete corbels without shear reinforcement, *Journal of the Institution of Engineers*, **84**, 202–212.

Lv, Y., Cheng, H., Ma, Z. (2012). Fatigue performances of glass fiber reinforced concrete in flexure, *Procedia Engineering*, **31**, 550–556.

Marikunte, S., Aldea, C., Shah, S. P. (1997). Durability of glass fiber reinforced cement composites : effect of silica fume and metakaolin, *Advanced Cement Based Materials,* **5**, 100–108.

Mast, R. F. (1968). Auxiliary reinforcement in concrete connections, *Journal of the Structural Division*, **94**(6), 1485–1504.

Mattock, A., Johal, L., Chow, H. (1975). Shear transfer in reinforced concrete with moment or tension acting across the shear plane, *PCI Journal*, **20**(4), 76–93.

Mirza, F. A., Soroushian, P. (2002). Effects of alkali-resistant glass fiber reinforcement on crack and temperature resistance of lightweight concrete, *Cement and Concrete Composites*, **24**, 223–227.

Mohammadi, Y., Singh, S. P., Kaushik, S. K. (2008). Properties of steel fibrous concrete containing mixed fibres in fresh and hardened state, *Construction and Building Materials*, **22**(5), 956–965.

Nanni, A. (1991). Fatigue behaviour of steel fiber reinforced concrete, *Cement and Concrete Composites*, **13**(4), 239–245.

NEAL, W. (1978). Glass fiber reinforced concrete (GFRC) — A new composite for construction. Available at: http://www.concreteconstruction.net.

Niedenhoff, G. F. H. (1963). The Reinforcement of Brackets and Short Deep Beams, a Translation of the Article in German That Appeared in *"Beton -Und Stahlbetonbau,"* **58**(5), 112–120.

Roth, M. J., Eamon, C. D., Slawson, T. R., Tonyan, T. D., Dubey, A. (2010). Ultra-high-strength glass fiber-reinforced concrete : mechanical behavior and numerical modeling, *ACI Materials Journal*, **107**, 185-194.

Shah, A. (2009). Evaluation of shear strength of high strength concrete beams evaluation of shear strength of high strength concrete beams, *The Arabian Journal for Science and Engineering*, **34**, 27–36.

Shakor, E. P. N., Pimplikar, P. S. S. (2011). Glass fibre reinforced concrete use in construction, *International Journal of Technology and Engineering System,* **2**(2), 12–18.

Siao, W. Bin. (1994). Shear strength of short reinforced concrete walls, corbels, and deep beams, *ACI Structural Journal*, **91**(2), 123–132.

Tamás Deák and Tibor Czigány. (2009). Chemical composition and mechanical properties of basalt and glass fibers: A comparison, *Textile Research Journal*, **79**(7), 645–651.

Tassew, S. T., Lubell, A. S. (2014). Mechanical properties of glass fiber reinforced ceramic concrete, *Construction and Building Materials*, **51**, 215–224.

William D. Cook, D. M. (1988). Studies of disturbed regions near discontinuities in reinforced concrete members, *ACI Structural Journal*, **85**(2), 206–216.

Yang, J., Lee, J., Min, K., Yoon, Y. (2008). Evaluating structural performance of high-strength concrete corbels containing steel and polypropylene fibers, *Journal of the Korea Concrete Institute*, **20**(6), 747–754.